



LJMU Research Online

Shaw, TA, Plater, AJ, Kirby, JR, Roy, K, Holgate, S, Tutman, P, Cahill, N and Horton, BP

Tectonic influences on late Holocene relative sea levels from the central-eastern Adriatic coast of Croatia

<http://researchonline.ljmu.ac.uk/id/eprint/9541/>

Article

Citation (please note it is advisable to refer to the publisher's version if you intend to cite from this work)

Shaw, TA, Plater, AJ, Kirby, JR, Roy, K, Holgate, S, Tutman, P, Cahill, N and Horton, BP (2018) Tectonic influences on late Holocene relative sea levels from the central-eastern Adriatic coast of Croatia. Quaternary Science Reviews. 200. pp. 262-275. ISSN 0277-3791

LJMU has developed **LJMU Research Online** for users to access the research output of the University more effectively. Copyright © and Moral Rights for the papers on this site are retained by the individual authors and/or other copyright owners. Users may download and/or print one copy of any article(s) in LJMU Research Online to facilitate their private study or for non-commercial research. You may not engage in further distribution of the material or use it for any profit-making activities or any commercial gain.

The version presented here may differ from the published version or from the version of the record. Please see the repository URL above for details on accessing the published version and note that access may require a subscription.

For more information please contact researchonline@ljmu.ac.uk

<http://researchonline.ljmu.ac.uk/>

1 **Tectonic influences on late Holocene relative sea levels from the central-**
2 **eastern Adriatic coast of Croatia.**

3

4 Timothy A. Shaw ^{a,*}, Andrew J. Plater ^b, Jason R. Kirby ^c, Keven Roy ^a, Simon Holgate ^d, Pero
5 Tutman ^e, Niamh Cahill ^f, Benjamin P. Horton ^{a, g}

6 ^a Asian School of the Environment, Nanyang Technological University, Singapore 639798,
7 Singapore.

8 ^b Department of Geography and Planning, School of Environmental Sciences, University of
9 Liverpool, Roxby Building, Liverpool, Merseyside L69 7ZT, U.K.

10 ^c School of Natural Sciences and Psychology, Liverpool John Moores University, Liverpool,
11 Merseyside, L3 3AF, U.K.

12 ^d Sea Level Research Ltd, Studio D, Baltic Creative Campus, Liverpool, Merseyside, L1 0AH,
13 U.K.

14 ^e Institute of Oceanography and Fisheries, Šetalište Ivana Meštrovića 63, 21000, Split, Croatia.

15 ^f School of Mathematics and Statistics, University College Dublin, Dublin, Ireland.

16 ^g Earth Observatory of Singapore, Nanyang Technological University, Singapore 639798,
17 Singapore.

18 * Corresponding author email: tshaw@ntu.edu.sg

19

20 **Abstract**

21 Differential tectonic activity is a key factor responsible for variable relative sea-level (RSL)
22 changes during the late Holocene in the Adriatic. Here, we compare reconstructions of RSL from

23 the central-eastern Adriatic coast of Croatia with ICE-7G_NA (VM7) glacial-isostatic model RSL
24 predictions to assess underlying driving mechanisms of RSL change during the past ~ 2700 years.
25 Local standardized published sea-level index points (n= 23) were combined with a new salt-marsh
26 RSL reconstruction and tide-gauge measurements. We enumerated fossil foraminifera from a short
27 salt-marsh sediment core constrained vertically by modern foraminiferal distributions, and
28 temporally by radiometric analyses providing sub-century resolution within a Bayesian age-depth
29 framework. We modelled changes in RSL using an Errors-In-Variables Integrated Gaussian
30 Process (EIV-IGP) model with full consideration of the available uncertainty. Previously
31 established index points show RSL rising from -1.48 m at 715 BCE to -1.05 m by 100 CE at 0.52
32 mm/yr (-0.82-1.87 mm/yr). Between 500 and 1000 CE RSL was -0.7 m below present rising to -
33 0.25 m at 1700 CE. RSL rise decreased to a minimum rate of 0.13 mm/yr (-0.37-0.64 mm/yr) at ~
34 1450 CE. The salt-marsh reconstruction shows RSL rose ~ 0.28 m since the early 18th century at
35 an average rate of 0.95 mm/yr. Magnitudes and rates of RSL change during the twentieth century
36 are concurrent with long-term tide-gauge measurements, with a rise of ~ 1.1 mm/yr. Predictions
37 of RSL from the ICE-7G_NA (VM7) glacial-isostatic model (-0.25 m at 715 BCE) are consistently
38 higher than the reconstruction (-1.48 m at 715 BCE) during the Late Holocene suggesting a
39 subsidence rate of 0.45 ± 0.6 mm/yr. The new salt-marsh reconstruction and regional index points
40 coupled with glacial-isostatic and statistical models estimate the magnitude and rate of RSL change
41 and subsidence caused by the Adriatic tectonic framework.

42

43 **Keywords:** Sea Level Changes; Adriatic; Croatia; late Holocene; Glacial isostatic adjustment;
44 Tectonic subsidence; Salt marsh; Foraminifera.

45

46 **1. Introduction**

47 Significant efforts have been made towards understanding Holocene relative sea-level (RSL)
48 changes in the Mediterranean (e.g., Flemming, 1969; Pirazzoli, 1976, 1991, 1996; Flemming and
49 Webb, 1986; Zerbini et al., 1996, 2017; Woodworth, 2003; Lambeck et al., 2004a; Marcos and
50 Tsimplis, 2008; Vacchi et al., 2016). During the Holocene, geological records illustrate eustatic
51 and glacio-hydro-isostatic changes (e.g., Lambeck and Purcell, 2005; Stocchi and Spada, 2007,
52 2009; Roy and Peltier, 2018) superposed by tectonic and local processes (e.g., Pirazzoli, 2005;
53 Antonioli et al., 2009, 2011; Vacchi et al., 2016). Indeed, tectonic effects on late Holocene RSL
54 histories in the northern Adriatic are particularly important, attesting to variable subsidence and
55 uplift rates (e.g., Benac et al., 2004, 2008; Furlani et al., 2011; Surić et al., 2014; Fontana et al.,
56 2017). The effect of tectonics on RSL histories in the central-eastern Adriatic is, however, less
57 well constrained (e.g. Faivre et al., 2013). Anthropogenic forcings since the mid to late 19th century
58 have contributed towards sea-level changes (e.g. Jevrejeva et al., 2009; Dangendorf et al., 2015;
59 Kopp et al., 2016). In the Adriatic and wider Mediterranean region, tide-gauge stations document
60 coherent RSL trends, simultaneously recording large inter-annual and inter-decadal variability
61 (Orlić and Pasarić, 2000; Tsimplis and Baker, 2000; Tsimplis and Josey, 2001; Tsimplis et al.,
62 2012). Comparing independent RSL datasets with differing resolution and time periods is,
63 therefore, problematic and restricts our understanding of RSL changes in the Adriatic.

64

65 Here, we reconstruct late Holocene RSL using geological and tide-gauge data coupled with a new
66 salt-marsh based reconstruction from the central-eastern coast of Croatia that bridges the gap
67 between late Holocene and modern sea-level data. Salt-marsh environments afford a unique ability
68 providing near continuous, decimeter vertical (Scott and Medioli, 1978, 1980; Horton and

69 Edwards, 2006) and sub-century temporal resolution (Törnqvist et al., 2015; Corbett and Walsh,
70 2015; Marshall, 2015). Their use in reconstructing RSL is well established across regions in
71 Northern (Gehrels et al., 2005; Kemp et al., 2013; Barlow et al., 2014; Saher et al., 2015) and
72 Southern Hemispheres (Gehrels et al., 2008; 2012; Strachan et al., 2014). Salt-marsh based
73 reconstructions have aided our understanding of climate-sea-level connections (Kemp et al., 2011;
74 Kopp et al., 2016); the onset of increases in the rate of RSL rise in the mid to late 19th century
75 (Kopp et al., 2016); and tectonic (van de Plassche et al., 2014), compaction (Brain et al., 2017)
76 and tidal range (Horton et al., 2013) influences on local RSL change. The Adriatic and wider
77 Mediterranean region, however, have evaded similar high-resolution RSL studies.

78

79 To better understand driving mechanisms of RSL change in the central-eastern Adriatic, we
80 compare the composite RSL record with ICE-7G_NA (VM7) glacio-isostatic model predictions
81 (Roy and Peltier, 2017) for the last ~ 2700 years. We show the magnitude of RSL change during
82 this period is offset to model predictions by more than 1 m, implying an overarching influence of
83 tectonic subsidence on RSL changes. We demonstrate the utility of the salt-marsh reconstruction
84 in deriving similar magnitudes and rates of RSL change to long-term tide-gauges.

85

86 **2. Study area**

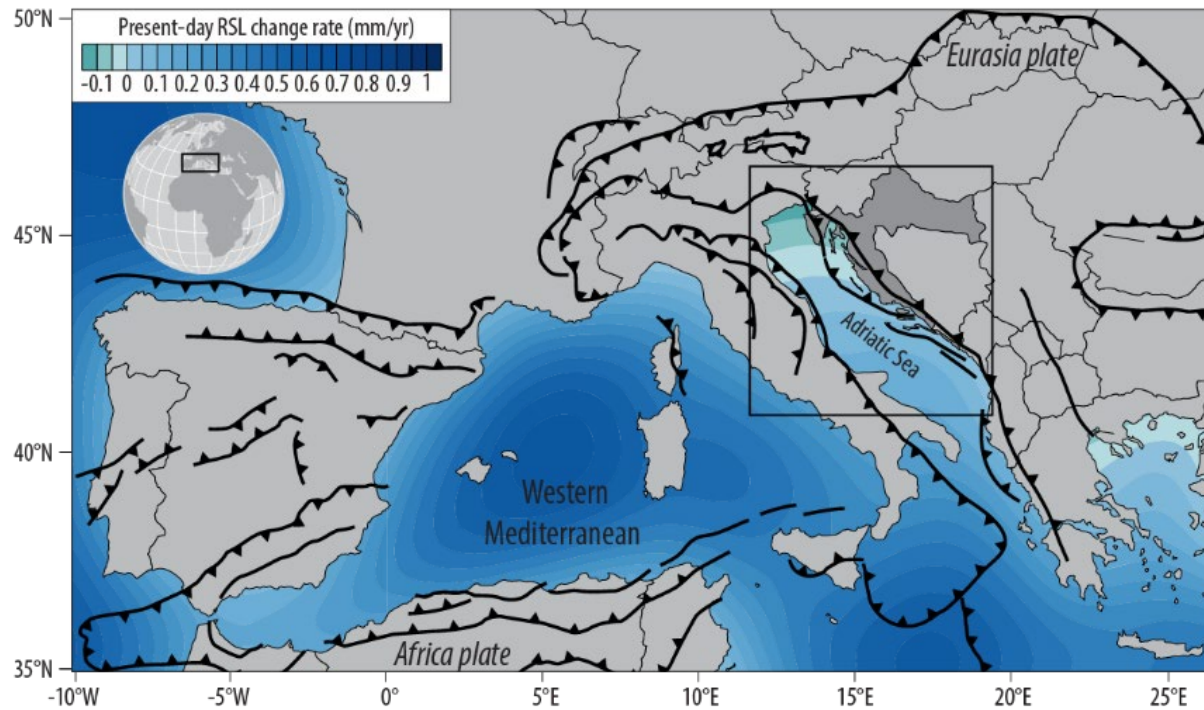
87 **2.1. Tectonic setting**

88 Tectonism in the western Mediterranean region is the consequence of the collision boundary
89 between the major tectonic plates of Africa and Eurasia (Fig. 1). This convergence zone results in
90 a number of microplates, including the Adriatic (McKenzie, 1972; Anderson and Jackson, 1987;
91 D'Agostino et al., 2008). The Adriatic microplate, which shows movements independent to Africa

92 and Eurasia (Grenerczy et al., 2005; Altiner et al., 2006; Serpelloni et al., 2013), is subdivided into
93 northern and southern sectors with the southern sector moving counterclockwise in a N-NW
94 direction at 5-10 mm/yr (Oldow et al., 2002; Herak et al., 2005; Marjanović et al., 2012). Tectonic
95 activity predominately occurs along the coasts and a through a number of fault lines that pass
96 through the region (Herak et al., 1996; 2017; Korbar, 2009). The distribution of earthquake
97 epicenters in the Adriatic between the Ancona-Zadar and Gargano-Dubrovnik lines (Fig. 2)
98 suggests this region is seismically more intense compared to the north with four $M_L \geq 5.5$ events
99 recorded since the twentieth century (Herak et al., 2005). Most recently, a sequence of earthquakes
100 peaking at $M_L = 5.5$ occurred in 2003 at Jabuka, some ~ 90 km west of Vis (Fig. 2) in the central
101 Adriatic Sea (Herak et al., 2005).

102

103 Modern measurements from Global Positioning System (GPS) stations reveal both lateral and
104 vertical land movements in the Adriatic region (Buble et al., 2010; Weber et al., 2010; Serpelloni
105 et al., 2013; Devoti et al., 2017). Vertical velocities from GPS stations in the north-western Adriatic
106 show significant subsidence rates up to ~ 8 mm/yr near the Po River Delta, reflecting crustal
107 movements and also compaction of sediments (Carminati et al., 2003; Antonioli et al., 2009).
108 While the density of observations along the eastern Adriatic are limited, vertical motions in
109 northern and central Croatia are close to 0 mm/yr with minor subsidence up to 1 mm/yr recorded
110 in the south near to Dubrovnik (Fig. 2).



111
 112 **Fig. 1.** Western Mediterranean showing location of major tectonic boundaries modified after
 113 Faccenna et al. (2014) with ICE-7G_NA (VM7) (Roy and Peltier, 2017) model predictions of
 114 present-day RSL change rate (mm/yr). Square outline depicts Adriatic study region presented in
 115 Fig. 2.

116
 117 **2.2. Oceanographic setting**

118 The Adriatic Sea is a relatively shallow elongated basin communicating with the Mediterranean
 119 Sea through the Strait of Otranto. The bathymetry is subdivided with a shallow (average ~ 35 m
 120 water depth) northern section near the Gulf of Trieste, progressively deepening to ~ 1200 m
 121 towards the south near Dubrovnik (Ciabatti et al., 1987; Orlić et al., 1992). Tidal ranges in the
 122 region are microtidal, increasing as water depth decreases to the north (Cushman-Roisin and
 123 Naimie, 2002). The influence of strong north-easterly Bora and south-easterly Sirocco winds can

124 significantly alter the tidal regime (Orlić et al., 1994; Vilibić, 2006; Ferla et al., 2007) and
125 meteorological tsunamis associated with prolonged low atmospheric pressure systems are a
126 relatively common occurrence (Vilibić and Šepić, 2009; Vilibić et al., 2017).

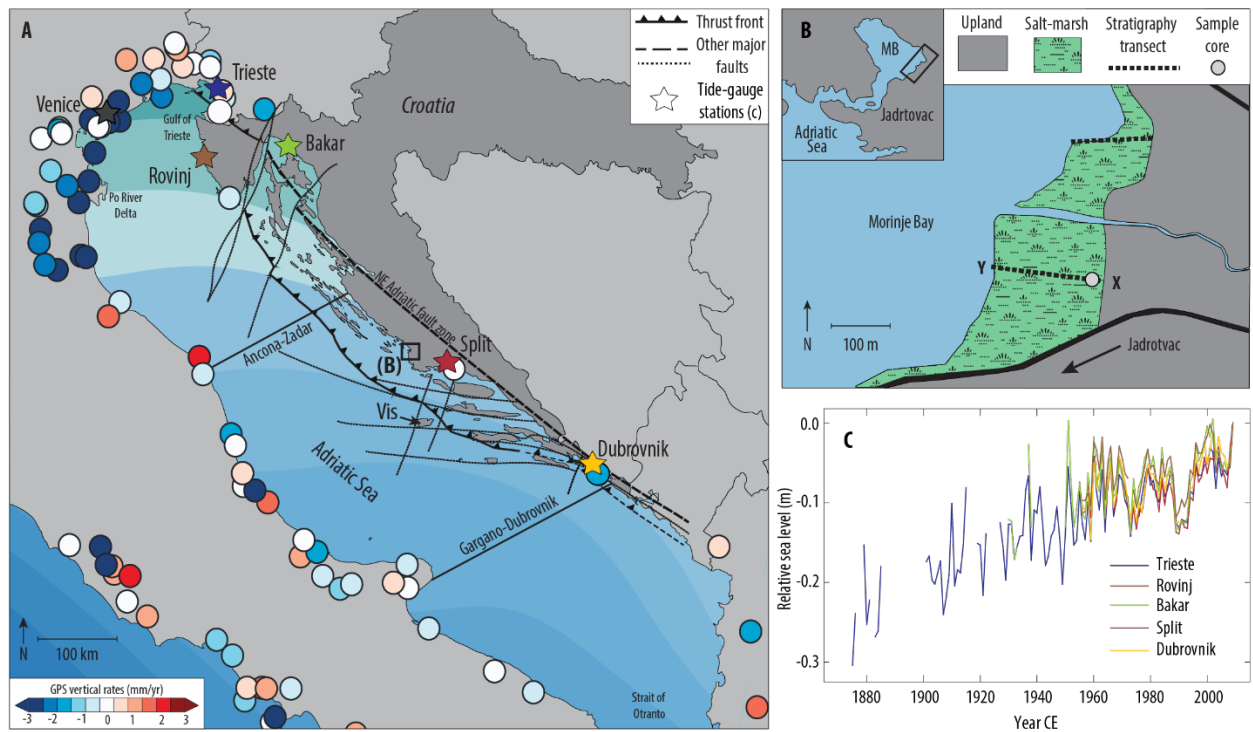
127
128 Instrumental observations of RSL change from long-term (>50 years) tide-gauge stations in the
129 Adriatic are restricted to the northern and eastern coastline (Fig. 2). The tidal station at Trieste
130 provides an inference of RSL change since the late 19th century while Bakar extends
131 (discontinuously) to 1930 CE. The tidal stations at Split and Dubrovnik extend to the mid-1950s.
132 By comparison to the rest of the Adriatic, high rates of RSL change are observed in the north in
133 Venice; however, this is attributable to anthropogenic influences exacerbating subsidence in the
134 region (Woodworth, 2003) as illustrated by the GPS network.

135

136 **2.3. Study site**

137 We investigated the salt-marsh environments located near Jadrtovac, along the central-eastern
138 Adriatic coastline of Croatia (Fig. 2). Our focus on this region was motivated by the availability
139 of pristine salt marshes (Pandža et al., 2007) and nearby long-term tide-gauge stations. In this
140 context, tide gauges can provide a means of self-evaluation for proxy-based reconstructions,
141 permitting independent comparison of RSL changes (e.g. Donnelly et al., 2004; Gehrels et al.,
142 2005; Kemp et al., 2009). Shaw et al. (2016) previously documented the vertical zonation of
143 contemporary foraminiferal assemblages at Jadrtovac, underpinning their potential to reconstruct
144 RSL change. The microtidal regime, with a mean tidal range of 0.23 m (Hydrographic Institute,
145 1955; Vilibić et al., 2005), also helps limit vertical uncertainties (Barlow et al., 2013). The salt-
146 marsh environment is located at the head of a ~ 2.5 km channel in the Morinje Bay, northwest of

147 Split and is a typical karstic environment with limited vegetation and poor soils on the surrounding
 148 slopes. The bay was infilled during the Holocene marine transgression, resulting in ~ 4.5 m of
 149 sediment (Bačani et al., 2004; Šparica et al., 2005). The main salt-marsh surface is ~ 130 m wide
 150 on the eastern side and gradually thins moving north around the bay.



151
 152 **Fig. 2.** (A) Adriatic study area showing the location of long-term (>50 years) tide-gauge stations
 153 (stars), the vertical land movements recorded by GPS stations (dots) modified after Serpelloni et
 154 al. (2013) and the simplified tectonic setting of the Croatian coastline modified after Korbar
 155 (2009), together with the location of Island of Vis and the Ancona-Zadar and Gargano-Dubrovnik
 156 lines (Herak et al., 2005) referred to in text. (B) Sample site at Jadrtovac within the Morinje Bay
 157 showing stratigraphic transects and sample core location. (C) Tide-gauge measurements of relative
 158 sea-level (RSL) change from stations highlighted in panel A.

159

160 3. Methodology

161 We investigated the depositional history of the salt-marsh environment, describing the underlying
162 lithostratigraphy according to the Troëls-Smith (1955) classification of coastal sediments. Core
163 transects were established capturing the full range of sub-environments from the landward high
164 salt-marsh (hereafter termed ‘high-marsh’) edge to open water boundary. Following this, a short
165 42 cm core (43.6803 N, 15.9570 E) was selected from the high-marsh and extracted using a 1 m-
166 long Eijkelkamp hand gouge corer with a diameter of 50 mm. The relative thinness of organic salt-
167 marsh deposits in the Morinje Bay most likely reflects low biological productivity and suspended
168 sediment concentrations in the tidal waters related to the impoverished soils in the limestone
169 catchment area. Nonetheless, the shallow core depth helps minimize the effects of post-
170 depositional lowering through sediment compaction (e.g. Brain et al., 2011) because of the limited
171 depth of overburden (e.g. Törnqvist et al., 2008; Horton and Shennan, 2009) and was drilled onto
172 the limestone bedrock. The outer surface of the core was carefully cleaned to prevent
173 contamination prior to sub-sampling of the undisturbed internal section and samples were kept
174 refrigerated until ready for analysis. We surveyed core sample altitudes using Real Time Kinetic
175 (RTK) satellite navigation and Leica Na820 optical leveling equipment relative to Croatian
176 national geodetic datum (m HVRS71).

177

178 Core samples were prepared at 1 cm intervals for all subsequent analyses. Samples for
179 foraminiferal analysis followed procedures outlined in Horton and Edwards (2006), enumerating
180 foraminiferal tests from sediments between sieve fractions 500 μm and 63 μm transferred to a wet
181 splitter (Scott and Hermelin, 1993) and analyzed wet under a binocular microscope. Our taxonomic
182 identification follows Shaw et al. (2016) where fossil foraminiferal assemblages mirrored those

183 observed in the contemporary environments and are typical of intertidal environments (Edwards
184 and Wright, 2015). Calcareous taxa *Ammonia*, *Elphidium* and *Quinqueloculina* were recorded as
185 generic groups (Horton and Edwards, 2006) and followed contemporary studies (Shaw et al.,
186 2016).

187

188 We determined the organic matter content of core sediments through Loss-On-Ignition (LOI)
189 (Ball, 1964), combusting sediment samples at 450°C for four hours to provide supplementary
190 evidence for intertidal environmental change (Plater et al., 2015).

191

192 **3.1. Chronology**

193 We established sedimentation rates for the salt-marsh core using a composite chronology
194 combining Accelerator Mass Spectrometry (AMS) ¹⁴C dating coupled with short-lived
195 radionuclides (²¹⁰Pb, ²²⁶Ra, ¹³⁷Cs and ²⁴¹Am) for sediments deposited in the past 100 years or so
196 (Corbett and Walsh, 2015). Radionuclide activities were analyzed by direct gamma assay at the
197 University of Liverpool Environmental Radioactivity Laboratory. Prior to gamma assay, we
198 determined the dry bulk density of the sediment samples by freeze-drying and weighing. Samples
199 were then lightly disaggregated before being stored for three weeks to allow radioactive
200 equilibration. Samples were analyzed using Ortec HPGe GWL series well-type coaxial low
201 background intrinsic germanium detectors (Appleby et al., 1986). We corrected for the effect of
202 self-absorption of low energy γ -rays within the sample (Appleby and Oldfield, 1992) and ²¹⁰Pb
203 ages calculated using the Constant Rate of Supply (CRS) model (Appleby and Oldfield, 1978;
204 Appleby et al., 1979). To further constrain ages obtained via ²¹⁰Pb dating, ¹³⁷Cs activities

205 referenced to nuclear weapons testing and the Chernobyl disaster were used as a chronological
206 marker (Appleby, 2001).

207

208 We selected plant macrofossils for AMS ^{14}C dating as opposed to bulk sediment dating for
209 improved accuracy and reduced uncertainties (Törnquist et al., 2015). Following preparation
210 methods outlined in Kemp et al. (2013b), we identified a varying abundance of *Scirpus*
211 *holoschoenus* seeds, a common high-marsh plant of the eastern Adriatic seaboard (Pandža et al.,
212 2007). Three, closely spaced intervals were selected for analysis by AMS ^{14}C at the NERC
213 Radiocarbon Facility, U.K (Table 2). Using *a priori* knowledge of their stratigraphic position (i.e.
214 the assumption that the lowest most sample was deposited before those above), conventional
215 radiocarbon ages were calibrated using the INTCAL13 calibration curve (Reimer et al., 2013)
216 within a Bayesian age-depth framework using Bchron (Haslett and Parnell, 2008; Parnell et al.,
217 2008) to provide 2σ age distributions.

218

219 **3.2. Reconstructing relative sea level**

220 Our assessment of late Holocene RSL changes in the central-eastern Adriatic are derived from
221 salt-marsh, tide-gauge and sea-level index points extracted from the quality controlled
222 Mediterranean Holocene RSL database of Vacchi et al. (2016). Indicative meanings of the proxy
223 RSL data are detailed in Table 1.

224

225 Our reconstruction of RSL changes from the salt-marsh environment uses indicative ranges from
226 contemporary foraminiferal distributions (Shaw et al., 2016) to provide estimates of the
227 paleommarsh elevation (PME) from fossil counterparts. We used stratigraphic markers of

228 environmental change (e.g., sediments and organic matter content) as supporting evidence. In
229 microtidal environments such as the Adriatic, using indicative ranges can derive an estimate of
230 PME with equivalent or improved precision over statistically more vigorous techniques (e.g.
231 transfer functions) (Kemp et al., 2017). We identified clusters in fossil foraminiferal assemblages
232 using Partitioning Around Medoids (PAM) cluster analysis (Kaufman and Rousseeuw, 1990) and
233 used contemporary distributions to provide an indicative range (i.e. vertical uncertainty) over
234 which the sample formed relative to mean tide level (MTL). To determine the most statistically
235 representative number of clusters, PAM produces silhouette widths providing a measure of the
236 samples classification. Our RSL reconstruction is restricted to the agglutinated assemblages only
237 within which chronologies and contemporary distributions are constrained. To attain RSL we
238 subtracted PME from surveyed sample elevations related to MTL (Shennan and Horton, 2002),
239 coupled with age estimations provided by the Bchron age-depth model.

240

241 We analyzed annual measurements from the Split Gradska tide-gauge spanning the period 1955 to
242 2009 CE. Tide-gauge measurements were analyzed relative to 2009 CE to directly compare RSL
243 changes with the core extraction date of the salt-mash reconstruction. Vertical uncertainties of the
244 tide gauge data were calculated from the standard deviation of annual measurements (± 0.03 m)
245 and a temporal uncertainty of ± 0.5 years follows that of Kemp et al. (2015).

246

247 We extracted Holocene sea-level index points ($n = 23$) from Vacchi et al. (2016) for the nearby
248 Island of Vis, central-eastern Adriatic (Fig. 2). These RSL data are based on fossil rims of
249 *Lithophyllum byssoides* (a precise fixed biological indicator of past RSL) and archaeological
250 evidence recorded by Faivre et al. (2013). Temporal uncertainties of the RSL data ranged from \pm

251 50 to 244 years with vertical uncertainties of ± 0.3 m. No reinterpretation of the RSL data was
252 applied after Vacchi et al. (2016).

253

254 **Table 1.** Indicative meanings of proxy RSL data used in RSL reconstruction.

Sea level indicator	Description	Indicative meaning
Salt-marsh	Organic sediment dominated by salt-marsh plant macrofossils and agglutinated foraminifera (e.g. <i>Entzia macrescens</i>).	MTL-HAT
* <i>Lithophyllum byssoides</i>	Fixed biological fossil rims of <i>Lithophyllum byssoides</i> recorded by Faivre et al. (2013).	MTL-HAT
*Archaeological	Functional interpretation of harbour structure (pier and dolia) recorded by Faivre et al. (2103).	MTL ± 0.25

255 MTL = mean tide level; HAT = highest astronomical tide. **Lithophyllum byssoides* and archaeological evidence
256 extracted from the Vacchi et al. (2016) Mediterranean RSL database.

257

258 We quantified RSL changes from the salt-marsh, instrumental and a composite RSL record using
259 an Error-In-Variables Integrated Gaussian Process (EIV-IGP) model (Cahill et al., 2015). The
260 EIV-IGP model takes an unevenly distributed RSL time series, prone to vertical and temporal
261 uncertainties, as input and produces estimates of RSL and rates of RSL with 95% credible
262 intervals. The EIV-IGP models rates of RSL change using a Gaussian process (GP) (Williams and
263 Rasmussen, 1996) and models RSL as the integral of the GP (IGP) plus (measured and estimated)
264 vertical uncertainty. Temporal uncertainties are accounted for by setting the IGP model in an
265 errors-in-variables (EIV) framework (Dey et al., 2000).

266

267 **3.3. Glacial-isostatic model predictions**

268 The Adriatic and wider Mediterranean has been a region of great interest in the study of the glacial-
269 isostatic adjustment (GIA) process. The large array of biological, archaeological and geological
270 indicators of past sea level have provided an opportunity to tune, test and/or validate GIA models
271 (e.g. Lambeck et al. 2004b; Lambeck & Purcell 2005; Stocchi & Spada 2009; Spada et al. 2009;
272 Lambeck et al. 2011; Vacchi et al. 2016). The recent availability of a standardized Holocene RSL
273 database covering the western Mediterranean basin (Vacchi et al., 2016) has enabled the
274 community to further test global models of the GIA process against RSL data, such as the ICE-
275 7G_NA (VM7) model (Roy & Peltier 2017; Roy & Peltier 2018).

276

277 Here, we compared the composite RSL record with glacial-isostatic model predictions in the
278 central-eastern Adriatic using the ICE-7G_NA (VM7) model (Roy and Peltier, 2017). Our model
279 choice is motivated by the ability of the ICE-7G_NA (VM7) model to explain a wide range of
280 geophysical observables related to the GIA process coming from geographically disparate regions
281 (covering formerly glaciated areas, forebulge regions and far-field sites) using a single, simple
282 rheological structure. This independence is important to understand patterns of sea-level evolution
283 in the context of complex local effects, such as tectonic activity (Antonioli et al., 2011). Indeed,
284 the ICE-7G_NA (VM7) model has been shown to fit a large proportion of the geographically and
285 temporally extensive RSL data set from Vacchi et al. (2016).

286

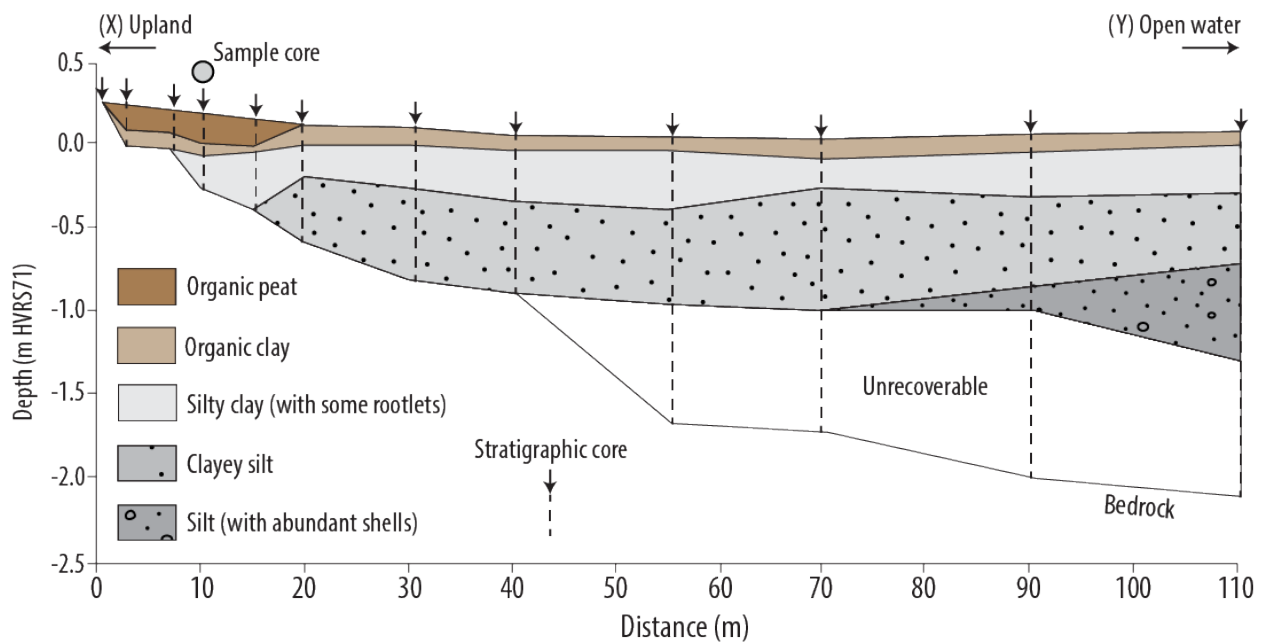
287 The ICE-7G_NA (VM7) model is an update to the precursor ICE-6G_C (VM5a) model of Peltier
288 et al. (2015). It includes a modified spherically-symmetric viscosity structure and an updated North
289 American ice-loading history, described in detail in Roy and Peltier (2017).

290

291 4. Results

292 4.1. Salt-marsh stratigraphy

293 Boreholes drilled across the salt-marsh showed an overall increase in sediment depth with distance
294 towards open water (Fig. 3). The lithostratigraphy revealed five main stratigraphic units where
295 sediment accumulation appeared relatively uniform across the site. An unrecoverable (i.e. overly
296 saturated) unit was found between 40 m and 110 m along the transect and overlain by varying silt
297 and clay units (often containing shells fragments) which become progressively more organic
298 towards the surface. An organic salt-marsh peat was restricted to the landward 20 m of the transect
299 where the sample core was extracted. The sediments in the sampled core were comprised of a silty
300 clay bottom unit with low organic content (LOI ~ 8%) between 42 cm and 20 cm. This was overlain
301 by an increasingly organic clay (LOI 10-40%) up to 11 cm and an organic humified peat deposit
302 towards the surface (LOI >50%) (Fig. 4).



303

304 **Fig. 3.** Simplified cross-sectional profile of the salt-marsh stratigraphy at Jadrtovac showing
305 location of sample core (see Fig. 2 for transect location).

306

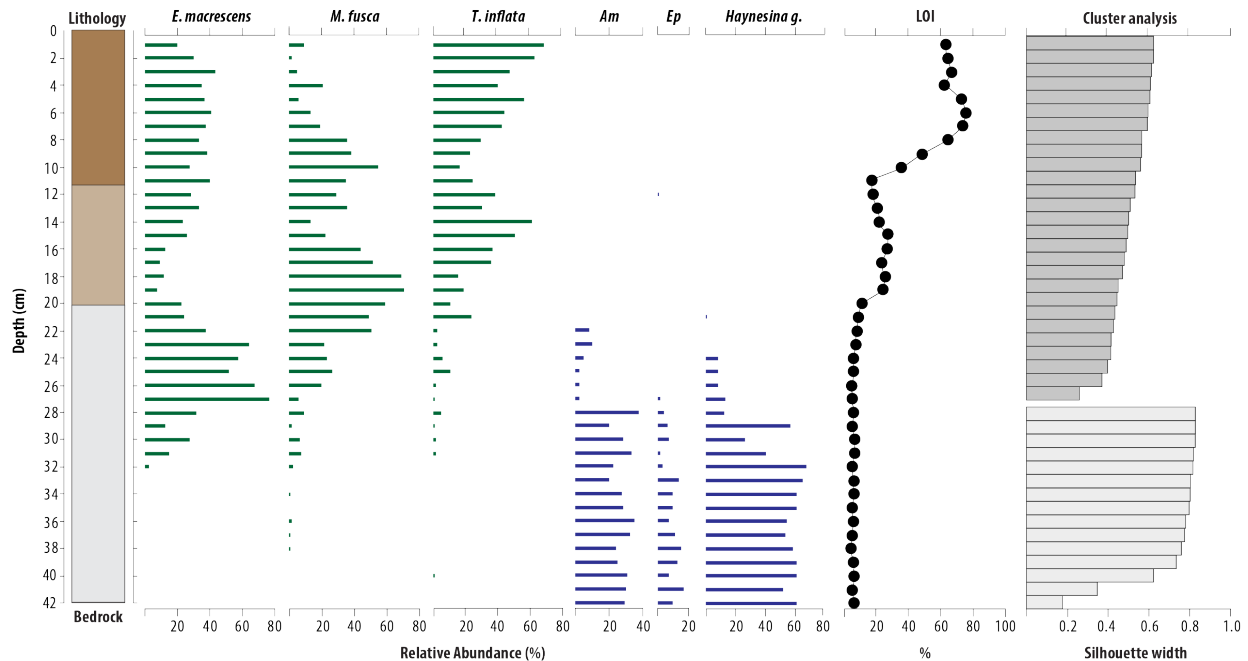
307 **4.2. Indicative meaning based on foraminiferal assemblages**

308 The biostratigraphy shows fossil foraminifera preserved throughout the entire sediment core
309 sequence (Fig. 4). An up-core transition from a calcareous-dominated assemblage to agglutinated
310 types is broadly coincident with a shift in sedimentation regime with progressively increasing
311 organic matter content at ~ 27 cm depth. Indeed, foraminiferal abundance was significantly higher
312 in line with this sedimentation change, with a mean abundance of 1310 per 5 cm³. Between 42 cm
313 and 32 cm, *Ammonia* spp., *Elphidium* spp. and *Haynesina germanica* dominate before agglutinated
314 types *Entzia macrescens*, *Miliammina fusca* and *Trochammina inflata* increase in relative
315 abundance. A decrease in the relative abundance of *M. fusca* from 19 cm (71%), corresponds with
316 an increase in *E. macrescens* and *T. inflata* towards the surface within the organic peat deposits
317 (LOI >40%).

318

319 Cluster analysis identified two foraminiferal assemblage groups in the fossil environment,
320 essentially discriminating between agglutinated and calcareous dominated assemblages, reflecting
321 the transition from intertidal muds and clays to organic salt-marsh sediments. Two broad indicative
322 meanings are appropriate given the current understanding of contemporary foraminiferal
323 distributions from the central-eastern Adriatic coast (e.g., Shaw et al., 2016). The fossil
324 foraminiferal assemblages mirrored those dominating the contemporary environment. The
325 contemporary distribution of agglutinated types (dominated by *E. macrescens* and *T. inflata*)
326 across the salt-marsh platform extends from 0.17 m ± 0.12 m MTL. Current vertical uncertainties

327 of ± 0.12 m using salt-marsh sediments are comparable to other RSL studies adopting different
 328 sea-level indicators from the central-eastern Adriatic (Vacchi et al., 2016).



329
 330 **Fig. 4.** Sample core sediment profile from Jadrtovac salt-marsh core showing lithology (following
 331 that displayed in Fig. 3), relative abundance (%) of the most abundant agglutinated (shaded green)
 332 and calcareous (shaded blue) foraminiferal taxa, organic matter content (LOI %) and results from
 333 cluster analysis. Foraminiferal taxa from left to right; *Entzia macrescens*; *Miliammina fusca*;
 334 *Trochammina inflata*; (*Am*) *Ammonia* spp., (*Ep*) *Elphidium* spp., *Haynesina germanica*.

335
 336 **4.3. Chronology**

337 We established age-depth relationships in the core through short-lived radionuclide analyses and
 338 AMS ^{14}C dating of three intervals between depths 25-30 cm where *Scirpus holoschoenus* seeds
 339 were observed within the calcareous-agglutinated foraminiferal assemblage transition (Table 2).
 340 The upper ~ 20 cm were constrained from downcore profiles of ^{210}Pb and ^{137}Cs , respectively (Fig.

341 5). Total ^{210}Pb activity reaches equilibrium with the supporting ^{226}Ra at ~ 20 cm depth.
 342 Unsupported ^{210}Pb concentrations record a minor discontinuity between 10-13 cm, below which
 343 they decline exponentially with depth. Analysis of ^{137}Cs activity shows a relatively well-defined
 344 maximum at 9-12 cm (69.9 Bq kg^{-1}). Its double peak reflects the same event that affected ^{210}Pb
 345 concentrations at this depth. As a result, the $^{137}\text{Cs}/^{210}\text{Pb}$ activity ratio can be a more accurate marker
 346 (Plater and Appleby, 2004) to show a well-defined peak between 10-12 cm that reflects peak
 347 fallout from the atmospheric testing of nuclear weapons (1963 CE). A second, more recent peak
 348 at 5-6 cm (57.1 Bq kg^{-1}), is interpreted as fallout from the Chernobyl reactor accident (1986 CE).

349

350 **Table 2.** Results from AMS ^{14}C analyses.

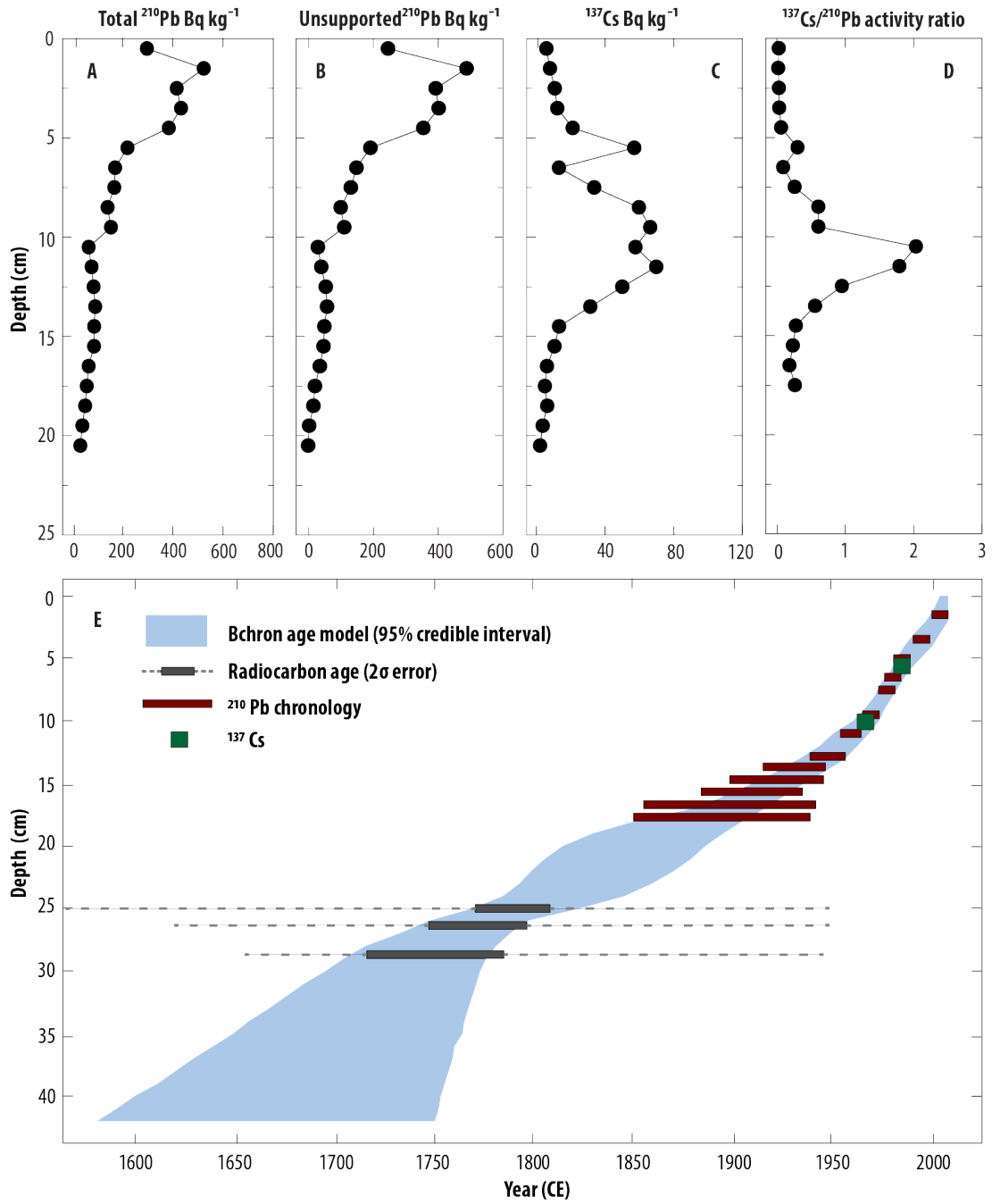
Depth (cm)	Laboratory code	^{14}C BP (\pm)	Year ($\delta^{13}\text{C}$ (‰))	Modelled (2σ) ^{14}C ages (CE)*	Material dated
25-26	SUERC45020	256 (37)	-25.3	1764-1805	<i>Scirpus holoschoenus</i> seeds
26-27	SUERC45021	213 (37)	-26.2	1742-1800	<i>Scirpus holoschoenus</i> seeds
28-30	SUERC45022	112 (37)	-26.8	1692-1784	<i>Scirpus holoschoenus</i> seeds

351 * ^{14}C ages calibrated within Bchron age-depth modelling software (Haslett and Parnell, 2008; Parnell et al., 2008).

352

353 Peaks in ^{137}Cs broadly correspond to those found from previous research in the Morinje Bay
 354 environment where maximum ^{137}Cs activity occurs within the upper 20 cm (Mihelčič et al., 2006).
 355 The CRS dating model place 1963 at 11.5 cm and 1986 at 5.5 cm, in good agreement with the
 356 depths suggested by the ^{137}Cs record. The results are relatively unambiguous down to ~ 16 cm,
 357 dated to 1920 CE beyond which the uncertainty of age estimates increases. The stratigraphic
 358 position of ^{14}C ages was used to constrain calibrated age distributions within Bchron. The

359 composite chronologies were modelled to provide age estimates with 95% credible intervals for
360 sediments in the upper 30 cm, with an average temporal uncertainty of ± 19 years (Fig. 5).

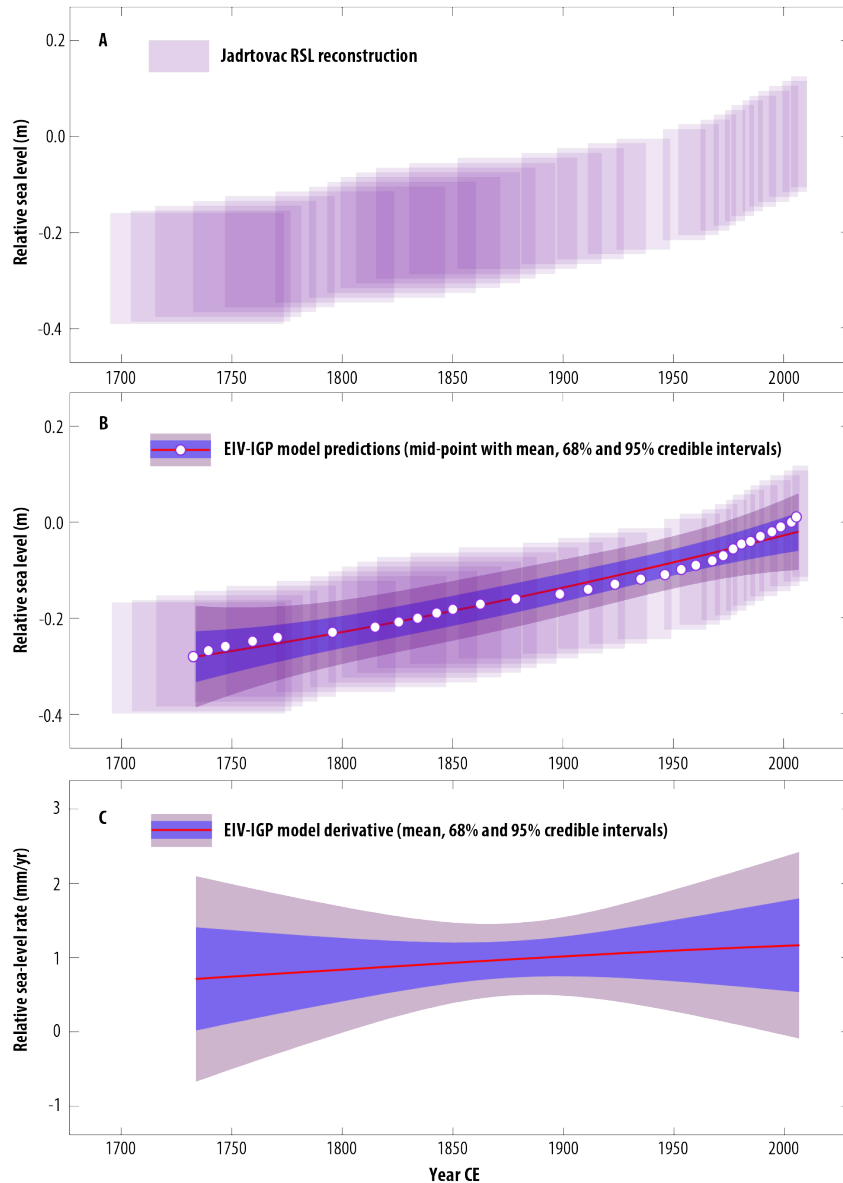


361

362 **Fig. 5.** Down-core profiles from short-lived radionuclide analyses (A-D) described in text. Error
363 bars from analyses are smaller than data point symbols used. (E) Bchron age-depth model with
364 95% credible interval incorporating short-lived radionuclide and AMS ^{14}C dating.

365 **4.4. Late Holocene relative sea-level trends**

366 Application of the EIV-IGP model to the salt-marsh RSL reconstruction showed a magnitude of
367 RSL change of ~ 0.28 m since 1733 CE (Fig. 6) with an average rate of RSL change of 0.95 mm/yr
368 over the whole record. Rates of RSL increase from 0.71 mm/yr (-0.67-2.09 mm/yr) to 0.93 mm/yr
369 (0.39-1.47 mm/yr) at 1850 CE when RSL was at -0.19 m below present level. Since 1900 CE, RSL
370 rose ~ 0.14 m at an average rate of 1.09 mm/yr, increasing to 1.16 mm/yr (-0.08-2.42 mm/yr) at
371 2009 CE.



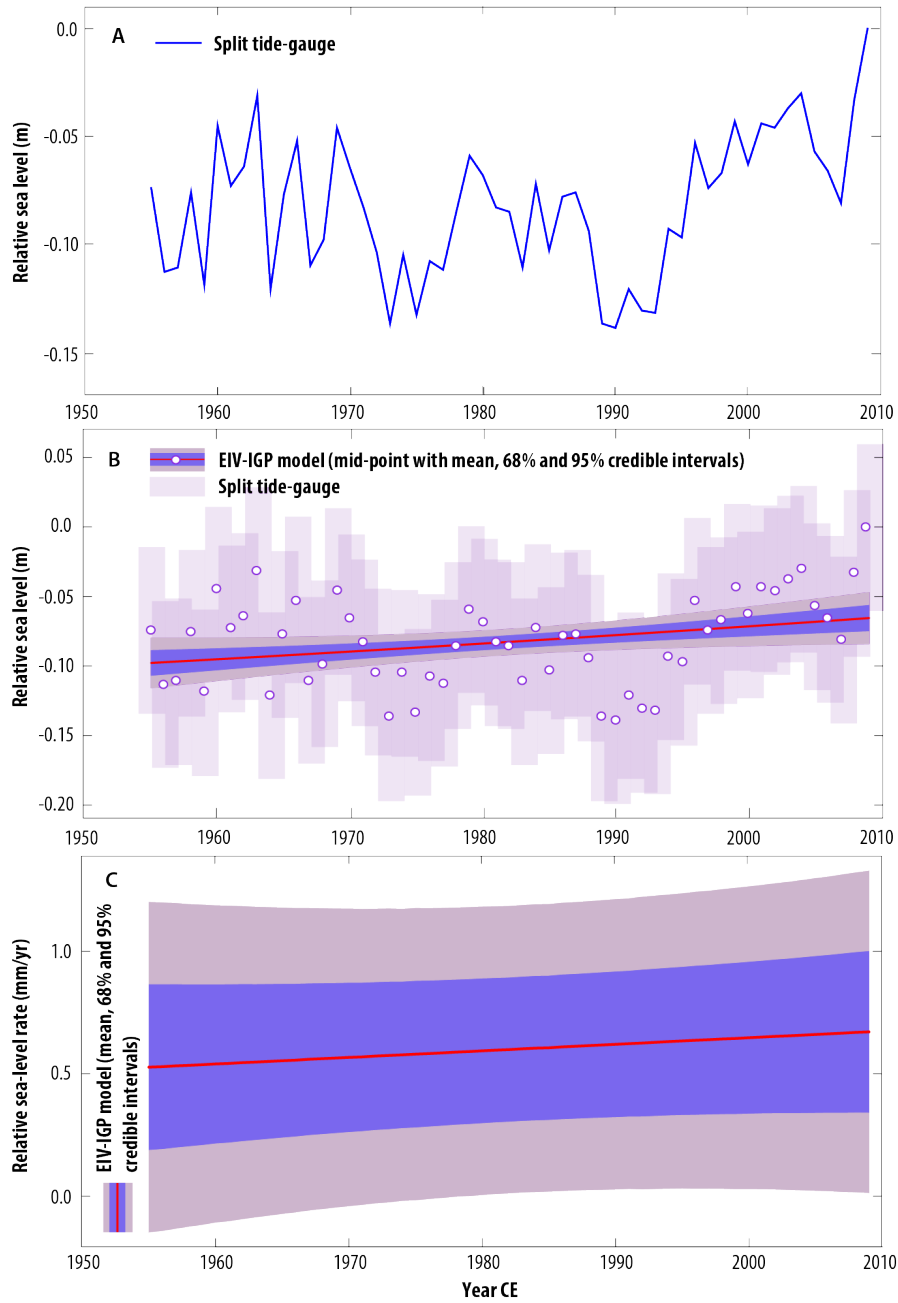
372

373 **Fig. 6.** (A) Reconstruction of relative sea-level (RSL) from salt-marsh core at Jadrtovac. (B) Error-
 374 In-Variables Integrated Gaussian Process (EIV-IGP) model showing mid-points from the RSL
 375 reconstruction with mean, 68% and 95% credible intervals. (C) Rates of RSL (mm/yr) with mean,
 376 68% and 95% credible intervals.

377

378 Annual measurements from the Split tide-gauge since 1955 CE show a magnitude RSL change of
 379 ~ 0.09 m (Fig. 7), concurrent with that recorded by salt-marsh sediments for the same period (\sim

380 0.08 m; Fig. 6). The average rate of RSL change was 0.60 mm/yr increasing from 0.52 mm/yr (-
 381 0.15-1.2 mm/yr) at 1955 CE to 0.67 mm/yr (0.01-1.33 mm/yr) at 2009 CE.



382
 383 **Fig. 7.** (A) Annual mean relative sea-level (RSL) trends from the Split Gradska tide-gauge (see
 384 Fig. 2 for location). (B) EIV-IGP model showing mid-points from tide-gauge measurements with
 385 mean, 68% and 95% credible intervals. (C) Rates of RSL (mm/yr) with mean, 68% and 95%

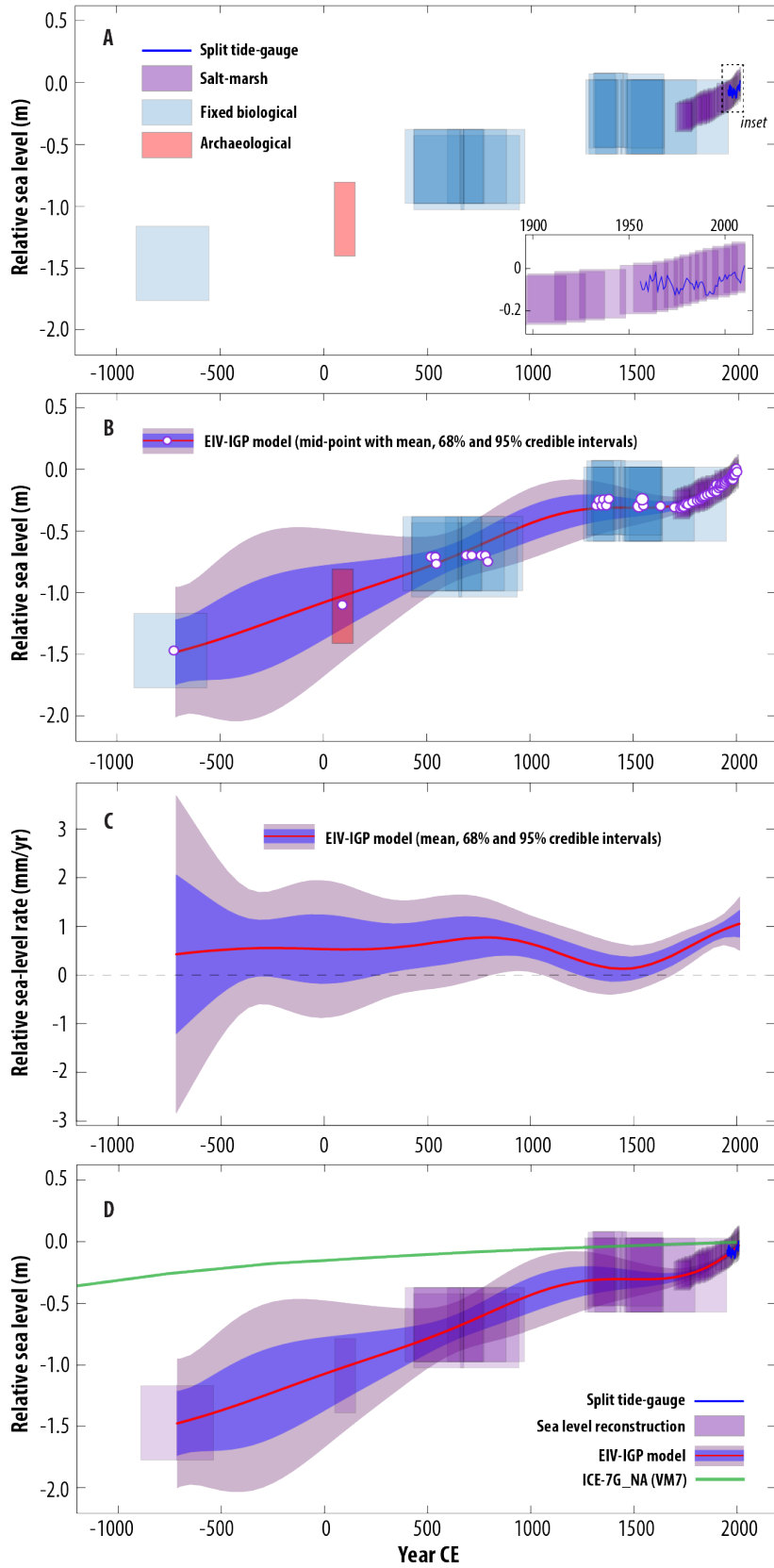
386 credible intervals. Annual RSL data accessed from the Permanent Service for Mean Sea Level on
387 13/11/2017 (<http://www.psmsl.org/products/trends/trends.txt>).

388

389 Late Holocene RSL data from the Island of Vis show a magnitude of RSL change of -1.48 m since
390 715 BCE increasing to -1.05 m by 100 CE at 0.52 mm/yr (-0.82-1.87 mm/yr) (Fig. 8). Between
391 500 and 1000 CE, RSL was at around -0.7 m below present increasing to -0.25 m at 1700 CE,
392 similar to that recorded by the salt-marsh reconstruction for the same time period (-0.28 m).
393 Acknowledging temporal paucity of earlier data, rates of RSL are relatively stable up to 800 CE
394 increasing to 0.77 mm/yr (-0.02-1.57 mm/yr) and then decreasing to 0.13 mm/yr (-0.37-0.64
395 mm/yr) at 1450 CE. The inclusion of the salt-marsh reconstruction and tide-gauge measurements
396 shows the gradual increase in RSL change towards the present.

397

398 Comparison of the late Holocene composite RSL record with ICE-7G_NA (VM7) model
399 predictions for the central-eastern Adriatic coast reveals a significant offset between the RSL data
400 and predicted results (Fig. 8d). At ~ 700 BCE, the ICE-7G_NA (VM7) model predicts RSL at -
401 0.25 m below present, compared to -1.48 ± 0.3 m suggested by the RSL data. Indeed, this offset is
402 manifest throughout the late Holocene towards the present, with the GIA model predicting
403 magnitudes of RSL changes lower than RSL reconstructions in the central-eastern Adriatic.



405 **Fig. 8.** (A) Late Holocene relative sea-level (RSL) change from fixed biological (*Lithophyllum*)
406 littoral rims and archaeological evidence from the Island of Vis recorded by Faivre et al. (2013),
407 the salt-marsh RSL reconstruction from Jadrtovac and Split Gradska tide-gauge measurements.
408 (B) Application of EIV-IGP model to the composite RSL showing mid-points with mean, 68%
409 and 95% credible intervals. (C) Rate of RSL (mm/yr) with mean, 68% and 95% credible intervals.
410 (D) Comparison of the composite RSL reconstruction against glacial-isostatic adjustment model
411 predictions of RSL from ICE-7G_NA (VM7) for the study region.

412

413 **5. Discussion**

414 Eustatic and glacio-hydro-isostatic processes have been important driving mechanisms of RSL
415 change in the Mediterranean (e.g., Lambeck and Purcell, 2005; Stocchi and Spada, 2007, 2009;
416 Roy and Peltier, 2018). At more local scales, particularly in the northern Adriatic, geological
417 evidence from geomorphological, sedimentological and archeological sea-level indicators have
418 been utilized to illustrate the importance of differential tectonic movements and local processes
419 (e.g. sediment compaction) affecting late Holocene RSL histories (e.g., Pirazzoli, 2005; Antonioli
420 et al., 2009, 2011; Marriner et al., 2014; Surić et al., 2014; Benjamin et al., 2017; Fontana et al.,
421 2017). Furthermore, understanding RSL changes from the late Holocene to the modern period have
422 been restricted by the temporal offset between geological and tide-gauge RSL records (Vacchi et
423 al., 2016), which record large inter-annual and inter-decadal variability (Tsimplis et al., 2012). Our
424 salt-marsh RSL reconstruction overcomes this limitation.

425

426 **5.1. Late Holocene relative sea levels in the Adriatic**

427 In the northwestern Adriatic, geomorphological and geoarchaeological evidence shows RSL was
428 at -2.0 ± 0.6 m between 1250-1110 BCE, increasing to -1.1 ± 0.3 m at ~ 50 BCE (Fontana et al.,
429 2017). In the northeastern Adriatic, archeological evidence shows RSL was between -1.75 and $-$
430 1.4 m ~ 0 CE (Vacchi et al., 2016). More recent RSL data from the Venice and Friuli lagoons
431 shows RSL was at -0.4 ± 0.6 m at ~ 1350 CE and below -0.3 m at 1650 CE (Vacchi et al., 2016).
432 These results compare well with our RSL data from the central-eastern Adriatic (Faivre et al.,
433 2013), which show a magnitude of RSL change of -1.48 ± 0.3 m since 715 BCE increasing to $-$
434 1.05 ± 0.3 m by ~ 100 CE and at -0.3 ± 0.3 m between 1350 and 1750 CE.

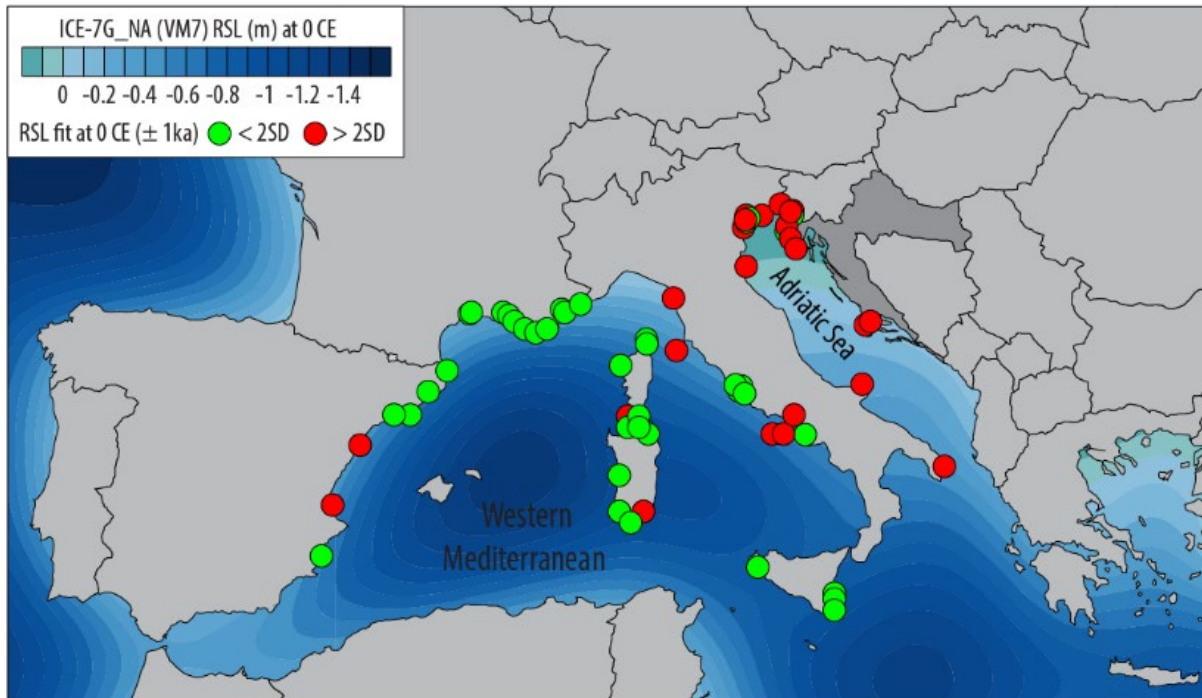
435

436 We compared the composite RSL record for the central-eastern Adriatic with glacio-isostatic
437 model predictions from ICE-7G_NA (VM7) (Roy and Peltier, 2017) (Fig. 8). The magnitude of
438 RSL change from the RSL data (1.48 ± 0.3 m), however, is significantly greater than ICE-7G_NA
439 (VM7) model predictions (0.25 m). If we assume the viscosity profile in the GIA model to be
440 accurate, the disparity between the RSL reconstructions and model predictions of RSL could be
441 due to eustatic input and/or tectonics in the absence of local processes (e.g., sediment compaction).
442 For example, the eustatic contribution to sea-level change during the late Holocene from the
443 Antarctic ice sheet may be underestimated in the ICE-7G_NA (VM7) model. Reconstructions of
444 RSL from the Mediterranean basin can play a crucial role in understanding the response of the
445 cryosphere to deglacial warming, in particular with respect to the late melting history of the
446 Antarctic ice sheet (Stocchi et al., 2009; Roy and Peltier, 2018). Indeed, one of the key distinctions
447 between various reconstructions of ice sheet deglaciation history lies in the late Holocene eustatic
448 component of sea-level change largely driven by the Antarctic and Greenlandic ice sheets.

449 Whereas the ICE-6G_C and ICE-7G_NA models of ice sheet loading history show around 2 m of
450 global mean sea level (GMSL) rise since 7ka, with no substantial increase after 4ka, other models
451 have inferred up to 6 m of GMSL rise since 7ka, with more than 80 cm of this change having
452 occurred after 4ka (Lambeck et al., 2014). It is important to place this observation in the broader
453 context of the quality of the fit provided by the ICE-7G_NA (VM7) to RSL data in the rest of the
454 western Mediterranean basin (Fig. 9). Roy and Peltier (2018) found their model to perform very
455 well in France, around the Ligurian Sea, in Corsica and in Sardinia. However, the authors identified
456 regions of sustained misfits between the model predictions and the Vacchi et al. (2016) database,
457 notably in central Spain, southwest Italy and in the Adriatic (Fig. 9). The GIA model is able to fit
458 the majority of RSL reconstructions between 3ka and 1ka in the western Mediterranean basin to
459 within two standard deviations. However, the RSL data that misfit with model predictions by
460 greater than two standard deviations are concentrated in the Adriatic.

461
462 The misfit between RSL data and model predictions provide support for the existence of tectonic
463 effects in the Adriatic, rather than an issue in the rate of GMSL rise included in the ICE-7G_NA
464 model. The difference between the reconstruction and the model suggest a tectonic subsidence of
465 0.45 ± 0.6 mm/yr. Although a full assessment of the influence of tectonics operating in the region
466 is challenging, the large variations in GPS vertical velocities (Fig. 2) observed around the Adriatic
467 Sea (Serpelloni et al., 2013) supports the idea of substantial tectonic motion. It should also be noted
468 that the presence of a complex tectonic setting should also be studied in the context of potential
469 local lateral heterogeneity in the viscosity of the mantle. Due to the small scale of the Adriatic Sea,
470 any sensitivity to such variations would be expected to be limited to the uppermost layers of the

471 mantle. Nonetheless, any rigorous determination of the geological evolution throughout the region
472 will need to consider these effects.



473
474 **Fig. 9.** Quality of the fit to the late Holocene RSL data from the western Mediterranean (Vacchi
475 et al., 2016) provided by the model predictions of the ICE-7G_NA (VM7) model, centered on 0
476 CE (± 1000 years). Green dots represent an agreement between the model prediction of RSL and
477 the local RSL reconstruction within 2 standard deviations (SD), while red dots indicate locations
478 where the difference between the model predictions and the RSL reconstruction is greater than 2
479 SD. Contours represent ICE-7G_NA (VM7) model predictions of RSL (m) at 0 CE.

480
481 The influence of local processes including paleotidal-range change and sediment compaction to
482 Holocene RSL histories (e.g. Horton et al., 2013) may also contribute to differences between
483 glacial-isostatic model predictions and RSL data. A lack of Mediterranean based studies currently
484 restricts the assessment of paleotidal-range changes (e.g. Hill et al., 2011; Griffiths and Hill, 2015)

485 to Mediterranean Holocene RSL data (e.g. Vacchi et al., 2016). However, given the local micro
486 tidal range and time period involved, we can consider the influence of paleotidal-range changes to
487 be negligible. Furthermore, the influence of sediment compaction, is also negligible due to the
488 limited depth of overburden (e.g. Törnqvist et al., 2008; Horton and Shennan, 2009) of the
489 relatively thin organic salt-marsh peat deposits at Jadrtovac. Nonetheless, future RSL studies in
490 the Adriatic and Mediterranean region accounting for these processes, would inherently provide
491 more accurate predictions of RSL change.

492

493 **5.2. Centennial scale relative sea level variability**

494 Climate-driven centennial sea-level variability superposed on late Holocene RSL are expressed at
495 the global scale (Kopp et al., 2016) with the transition from the Medieval Climate Anomaly (MCA)
496 to the Little Ice Age (LIA) coinciding with a reduction in air and ocean temperatures (Mann et al.,
497 2009; Marcott et al., 2013; Rosenthal et al., 2017). Application of the EIV-IGP model to the
498 geological data from Vis shows a (subtle) increase and decrease in RSL rate, occurring at 800 CE
499 and 1450 CE, respectively. This broadly coincides with the MCA to LIA transition which Faivre
500 et al. (2013) suggested a response of central-eastern Adriatic sea levels similar to the North Atlantic
501 based on comparisons of RSL trends with salt-marsh based RSL reconstructions from North
502 America (Kemp et al., 2011). While the temporal coverage and vertical resolution of late Holocene
503 RSL data from the western Mediterranean currently restricts more local interpretations (e.g.
504 Vacchi et al., 2016), variability of late Holocene RSL in the eastern Mediterranean has been
505 reported (Sivan et al., 2004). Archaeological and biological proxy data from Israel support
506 inferences for sea-level variability between 900 and 1300 CE (Toker et al., 2012). Indeed, the

507 climatic deterioration during the LIA has also been associated with a period of increased
508 storminess throughout the Mediterranean region (Marriner et al., 2017).

509

510 **5.3. Modern sea-level rise**

511 Empirical modelling of proxy and instrumental RSL records has enabled inferences regarding
512 timing the onset of modern sea-level rise (Kopp et al., 2016). At the global scale, sea levels began
513 rising around 1860 CE (Kemp et al., 2011; Kopp et al., 2016), synchronous with sustained
514 industrial-era warming of the tropical oceans and Northern Hemisphere continents (Abram et al.,
515 2016). Here, we applied the EIV-IGP model to our salt-marsh reconstruction, which captures the
516 dynamic evolution of sea-level change with robust consideration of sources of uncertainty (Cahill
517 et al., 2015). Importantly, the EIV-IGP model shows a subtle but constant increase in the mean
518 rate of RSL rise from 0.71 mm/yr (-0.67-2.09 mm/yr) to 1.16 mm/yr (-0.08-2.42 mm/yr) between
519 1733 CE and 2009 CE (Fig. 6c). Indeed, this subtle increase in mean RSL rate stems from the
520 deviation of sea-level trends recorded up to ~ 1450 CE (Fig. 8c).

521

522 Uncertainties in constraining age-depth relationships in the salt-marsh reconstruction during the
523 nineteenth century may preclude important inferences regarding timing of the onset of modern
524 RSL rise in the Mediterranean. Records of RSL change from twentieth century tide-gauge stations
525 in the Mediterranean show RSL rising at a rate of 1.1 to 1.3 mm/yr (Tsimplis and Baker, 2000;
526 Orlić and Pasarić, 2000; Marcos and Tsimplis, 2008). Zerbini et al. (2017) also report a rising RSL
527 trend of 1.2 to 1.3 mm/yr (\pm 0.2 to 0.5 mm/yr) from their analyses. The salt-marsh RSL
528 reconstruction supports these findings with an average RSL rate of ~ 1.1 mm/yr between 1900 and
529 2009. While a lower average rate of RSL change was recorded by the Split tide-gauge (0.60

530 mm/yr), this reflects a deviation of sea levels recorded by Adriatic and Mediterranean tide-gauge
531 stations during the latter half of the twentieth century. A decrease in RSL rate between 1960-1993
532 (Tsimplis and Baker, 2000; Marcos and Tsimplis, 2008) coincided with a period of higher
533 atmospheric pressure and evaporation over the basin driven by the high state of the North Atlantic
534 Oscillation (Tsimplis and Josey, 2001).

535

536 **6. Conclusions**

537 Reconstructions of RSL change along the central-eastern coast of Croatia offer new insight to the
538 late Holocene sea-level history of the central-eastern Adriatic region. We reconstructed RSL using
539 salt-marsh sediments and foraminifera that underpins their under-utilized potential to derive RSL
540 changes in the Mediterranean. Fossil foraminifera enumerated from a short sediment core were
541 constrained vertically by contemporary foraminiferal distributions, and temporally, by radiometric
542 dating techniques within a Bayesian age-depth framework. The reconstruction shows RSL rose ~
543 0.28 m since ~ 1733 CE, with a magnitude RSL change of ~ 0.14 m comparable to tide-gauge
544 records during the twentieth century. We modelled RSL changes using the EIV-IGP model (Cahill
545 et al., 2015) showing rates of RSL change increasing from 0.71 mm/yr (-0.67-2.09 mm/yr) at ~
546 1733 CE to 0.93 mm/yr (0.39-1.47 mm/yr) at 1850 CE. Average rates of RSL during the twentieth
547 century, rising at ~ 1.1 mm/yr, are analogous with the instrumental measurements.

548

549 We compared a composite RSL record combining the tide-gauge and salt-marsh reconstruction
550 with local published sea-level index points (n=23) (Faivre et al., 2013) against ICE-7G_NA (VM7)
551 glacio-isostatic model predictions (Roy and Peltier, 2017) for the last ~ 2700 years. The magnitude
552 of RSL change from the RSL reconstruction (1.48 m) differs from the glacio-isostatic model

553 prediction by more than 1 m, supporting subsidence rates driven by the Adriatic tectonic
554 framework of 0.45 ± 0.6 mm/yr. Application of the EIV-IGP model supports evidence for late
555 Holocene sea-level variability with rates of RSL rise decreasing from 0.77 mm/yr (-0.02-1.57
556 mm/yr) at 800 CE to 0.13 mm/yr (-0.37-0.64 mm/yr) at ~ 1450 CE. The temporal coverage of the
557 salt-marsh reconstruction bridging RSL changes from the late Holocene to the modern
558 instrumental period shows the gradual increase in mean RSL rate towards the present.

559

560 **Acknowledgements**

561 This research was supported by the National Environment Research Council (NERC) U.K. PhD
562 studentship award SR1686482, Singapore Ministry of Education Academic Research Fund Tier 1
563 RG119/17, National Research Foundation Singapore and the Singapore Ministry of Education
564 under the Research Centres of Excellence initiative. We gratefully acknowledge the NERC
565 radiocarbon steering committee for granting radiocarbon dating support (Allocation Number
566 1678.1012) and thank Peter Appleby, University of Liverpool, for the radionuclide analyses. This
567 article is a contribution to PALSEA2 (Palaeo-Constraints on Sea-Level Rise), International
568 Geoscience Program (IGCP) Project 639, “Sea Level Change from Minutes to Millennia,” and
569 INQUA Project 1601P “Geographic variability of HOLOCENE relative SEA level (HOLSEA).”
570 This work is Earth Observatory of Singapore contribution no. 204. We dedicate this paper to Peter
571 John Shaw.

572

573 **References**

- 574 Abram, N.J., McGregor, H.V., Tierney, J.E., Evans, M.N., McKay, N.P., Kaufman, D.S.,
575 Consortium, the P. 2k, Thirumalai, K., Martrat, B., Goosse, H., Phipps, S.J., Steig, E.J., Kilbourne,
576 K.H., Saenger, C.P., Zinke, J., Leduc, G., Addison, J.A., Mortyn, P.G., Seidenkrantz, M.-S., Sicre,
577 M.-A., Selvaraj, K., Filipsson, H.L., Neukom, R., Gergis, J., Curran, M.A.J., Gunten, L. von, 2016.
578 Early onset of industrial-era warming across the oceans and continents. *Nature* 536, 411.
579 <https://doi.org/10.1038/nature19082>
- 580 Altiner, Y., 2006. Present-day tectonics in and around the Adria plate inferred from GPS
581 measurements. *Special Paper of the Geological Society of America* 409.
582 [https://doi.org/10.1130/2006.2409\(03\)](https://doi.org/10.1130/2006.2409(03))
- 583 Anderson, H., Jackson, J., 1987. Active tectonics of the Adriatic Region. *Geophysical Journal of*
584 *the Royal Astronomical Society* 91, 937–98;3. <https://doi.org/10.1111/j.1365->
585 [246X.1987.tb01675.x](https://doi.org/10.1111/j.1365-246X.1987.tb01675.x)
- 586 Antonioli, F., Faivre, S., Ferranti, L., Monaco, C., 2011. Tectonic contribution to relative sea level
587 change. *Quaternary International* 232, 1–4. <https://doi.org/10.1016/j.quaint.2010.10.003>
- 588 Antonioli, F., Ferranti, L., Fontana, A., Amorosi, A., Bondesan, A., Braitenberg, C., Dutton, A.,
589 Fontolan, G., Furlani, S., Lambeck, K., Mastronuzzi, G., Monaco, C., Spada, G., Stocchi, P., 2009.
590 Holocene relative sea-level changes and vertical movements along the Italian and Istrian
591 coastlines. *Quaternary International* 206, 102–133. <https://doi.org/10.1016/j.quaint.2008.11.008>
- 592 Appleby, P.G., 2001. Chronostratigraphic Techniques in Recent Sediments, in: Last, W., Smol, J.
593 (Eds.), *Tracking Environmental Change Using Lake Sediments, Developments in*
594 *Paleoenvironmental Research*. KluwerAcademic Publishers, Dordrecht, pp. 171–203.

595 Appleby, P.G., Nolan, P.J., Gifford, D.W., Godfrey, M.J., Oldfield, F., Anderson, N.J., Battarbee,
596 R.W., 1986. ²¹⁰Pb dating by low background gamma counting. *Hydrobiologia* 143, 21–27.
597 <https://doi.org/10.1007/bf00026640>

598 Appleby, P.G., Oldfield, F., 1978. The calculation of lead-210 dates assuming a constant rate of
599 supply of unsupported ²¹⁰Pb to the sediment. *CATENA* 5, 1–8. <https://doi.org/10.1016/s0341->
600 8162(78)80002-2

601 Appleby, P.G., Oldfield, F., Thompson, R., Huttunens, P., Tolone, K., 1979. ²¹⁰Pb dating of
602 annually laminated lake sediments from Finland. *Nature* 280, 53–55.

603 Bačani, A., Koch, G., Bergant, S., Šparica, M., Viličić, D., Dolenc, T., Vreča, P., Ibrahimpašić,
604 H., 2004. Origin of Recent Organic-Rich Sediments from Morinje Bay (Northern Dalmatia,
605 Croatia): Aspects of Hydrological and Hydrogeological Impact. Abstracts, Scientific Sessions,
606 Part 2, 32nd International Geological Congress, Florence.

607 Ball, D.F., 1964. Loss-on-ignition as an estimate of organic matter and organic carbon in non-
608 calcareous soils. *Journal of Soil Science* 15, 84–92. <https://doi.org/10.1111/j.1365->
609 2389.1964.tb00247.x

610 Barlow, N.L.M., Long, A.J., Saher, M.H., Gehrels, W.R., Garnett, M.H., Scaife, R.G., 2014. Salt-
611 marsh reconstructions of relative sea-level change in the North Atlantic during the last 2000 years.
612 *Quaternary Science Reviews* 99, 1–16. <https://doi.org/10.1016/j.quascirev.2014.06.008>

613 Barlow, N.L.M., Shennan, I., Long, A.J., Gehrels, W.R., Saher, M.H., Woodroffe, S.A., Hillier,
614 C., 2013. Salt marshes as late Holocene tide gauges. *Global and Planetary Change* 106, 90–110.
615 <https://doi.org/10.1016/j.gloplacha.2013.03.003>

616 Benac, Č., Juračić, M., Bakran-Petricioli, T., 2004. Submerged tidal notches in the Rijeka Bay NE
617 Adriatic Sea: indicators of relative sea-level change and of recent tectonic movements. *Marine*
618 *Geology* 212, 21–33. <https://doi.org/10.1016/j.margeo.2004.09.002>

619 Benac, C., Juracic, M., Blaskovic, I., 2008. Tidal notches in Vinodol Channel and Bakar Bay, NE
620 Adriatic Sea: Indicators of recent tectonics. *Marine Geology* 248, 151–160.
621 <https://doi.org/10.1016/j.margeo.2007.10.010>

622 Benjamin, J., Rovere, A., Fontana, A., Furlani, S., Vacchi, M., Inglis, R.H., Galili, E., Antonioli,
623 F., Sivan, D., Miko, S., Mourtzas, N., Felja, I., Meredith-Williams, M., Goodman-Tchernov, B.,
624 Kolaiti, E., Anzidei, M., Gehrels, R., 2017. Late Quaternary sea-level changes and early human
625 societies in the central and eastern Mediterranean Basin: An interdisciplinary review. *Quaternary*
626 *International* 449, 29–57. <https://doi.org/10.1016/j.quaint.2017.06.025>

627 Brain, M.J., Kemp, A.C., Hawkes, A.D., Engelhart, S.E., Vane, C.H., Cahill, N., Hill, T.D.,
628 Donnelly, J.P., Horton, B.P., 2017. Exploring mechanisms of compaction in salt-marsh sediments
629 using Common Era relative sea-level reconstructions. *Quaternary Science Reviews* 167, 96–111.
630 <https://doi.org/10.1016/j.quascirev.2017.04.027>

631 Brain, M.J., Long, A.J., Petley, D.N., Horton, B.P., Allison, R.J., 2011. Compression behaviour of
632 minerogenic low energy intertidal sediments. *Sedimentary Geology* 233, 28–41.
633 <https://doi.org/10.1016/j.sedgeo.2010.10.005>

634 Buble, G., Bennett, R.A., Hreinsdóttir, S., 2010. Tide gauge and GPS measurements of crustal
635 motion and sea level rise along the eastern margin of Adria. *Journal of Geophysical Research* 115,
636 B02404. <https://doi.org/10.1029/2008jb006155>

637 Cahill, N., Kemp, A.C., Horton, B.P., Parnell, A.C., 2015. Modeling sea-level change using errors-
638 in-variables integrated Gaussian processes. *Ann. Appl. Stat.* 9, 547–571.
639 <https://doi.org/10.1214/15-AOAS824>

640 Carminati, E., Martinelli, G., Severi, P., 2003. Influence of glacial cycles and tectonics on natural
641 subsidence in the Po Plain (Northern Italy): Insights from ¹⁴C ages. *Geochemistry, Geophysics,*
642 *Geosystems* 4. <https://doi.org/10.1029/2002GC000481>

643 Ciabatti, M., Curzi, P., Ricci Lucchi, F. 1987. Quaternary sedimentation in the Central Adriatic
644 Sea. *Giornale di Geologia* 49, 113–125.

645 Corbett, D.R., Walsh, J. p., 2015. ²¹⁰Pb and ¹³⁷Cs, in: Shennan, I., Long, A.J., Horton,
646 B.P. (Eds.), *Handbook of Sea-Level Research*. John Wiley & Sons, Ltd, pp. 361–372.
647 <https://doi.org/10.1002/9781118452547.ch24>

648 Cushman-Roisin, B., Naimie, C.E., 2002. A 3D finite-element model of the Adriatic tides. *Journal*
649 *of Marine Systems* 37, 279–297. [https://doi.org/10.1016/S0924-7963\(02\)00204-X](https://doi.org/10.1016/S0924-7963(02)00204-X)

650 D’Agostino, N., Avallone, A., Cheloni, D., D’Anastasio, E., Mantenuto, S., Selvaggi, G., 2008.
651 Active tectonics of the Adriatic region from GPS and earthquake slip vectors. *J. Geophys. Res.*
652 113, B12413. <https://doi.org/10.1029/2008JB005860>

653 Dangendorf, S., Marcos, M., Müller, A., Zorita, E., Riva, R., Berk, K., Jensen, J., 2015. Detecting
654 anthropogenic footprints in sea level rise. *Nature Communications* 6, 7849.
655 <https://doi.org/10.1038/ncomms8849>

656 Devoti, R., D’Agostino, N., Serpelloni, E., Pietrantonio, G., Riguzzi, F., Avallone, A., Cavaliere,
657 A., Cheloni, D., Cecere, G., D’Ambrosio, C., Franco, L., Selvaggi, G., Metois, M., Esposito, A.,
658 Sepe, V., Galvani, A., Anzidei, M., 2017. A Combined Velocity Field of the Mediterranean
659 Region. *Ann. Geophys.* 60, S0215. <https://doi.org/10.4401/ag-7059>

660 Devy, D.K., Ghosh, S.K., Mallick, B.K., 2000. Generalized Linear Models: A Bayesian
661 Perspective. Marcel Dekker, New York.

662 Donnelly, J.P., Cleary, P., Newby, P., Ettinger, R., 2004. Coupling instrumental and geological
663 records of sea-level change: Evidence from southern New England of an increase in the rate of
664 sea-level rise in the late 19th century. *Geophysical Research Letters* 31, L05203.
665 <https://doi.org/10.1029/2003gl018933>

666 Edwards, R., Wright, A., 2015. Foraminifera, in: Shennan, I., Long, A.J., Horton, B.P. (Eds.),
667 Handbook of Sea-Level Research. John Wiley & Sons, Ltd, pp. 191–217.

668 Engelhart, S.E., Horton, B.P., 2012. Holocene sea level database for the Atlantic coast of the
669 United States. *Quaternary Science Reviews, Coastal Change during the Late Quaternary* 54, 12–
670 25. <https://doi.org/10.1016/j.quascirev.2011.09.013>

671 Faccenna, C., Becker, T.W., Auer, L., Billi, A., Boschi, L., Brun, J.P., Capitanio, F.A., Funiciello,
672 F., Horvath, F., Jolivet, L., Piromallo, C., Royden, L., Rossetti, F., Serpelloni, E., 2014. Mantle
673 dynamics in the Mediterranean. *Rev. Geophys.* 52, 2013RG000444.
674 <https://doi.org/10.1002/2013RG000444>

675 Faivre, S., Bakran-Petricioli, T., Horvatinčić, N., Sironić, A., 2013. Distinct phases of relative sea
676 level changes in the central Adriatic during the last 1500 years — influence of climatic variations?
677 *Palaeogeography, Palaeoclimatology, Palaeoecology* 369, 163–174.
678 <https://doi.org/10.1016/j.palaeo.2012.10.016>

679 Ferla, M., Cordella, M., Michielli, L., Rusconi, A., 2007. Long-term variations on sea level and
680 tidal regime in the lagoon of Venice. *Estuarine, Coastal and Shelf Science* 75, 214–222.
681 <https://doi.org/10.1016/j.ecss.2007.03.037>

682 Flemming, N.C., 1969. Archaeological Evidence for Eustatic Change of Sea Level and Earth
683 Movements in the Western Mediterranean During the Last 2,000 Years. Geological Society of
684 America Special Papers 109, 1–98. <https://doi.org/10.1130/SPE109-p1>

685 Flemming, N.C., Webb, C.O., 1986. Tectonic and eustatic coastal changes during the last 10,000
686 years derived from archaeological data. *Zeitschrift für Geomorphologie, Supplementband 62*, 1–
687 29.

688 Fontana, A., Vinci, G., Tasca, G., Mozzi, P., Vacchi, M., Bivi, G., Salvador, S., Rossato, S.,
689 Antonioli, F., Asioli, A., Bresolin, M., Di Mario, F., Hajdas, I., 2017. Lagoonal settlements and
690 relative sea level during Bronze Age in Northern Adriatic: Geoarchaeological evidence and
691 paleogeographic constraints. *Quaternary International, Quaternary coastal and marine studies in
692 Central Mediterranean 439*, 17–36. <https://doi.org/10.1016/j.quaint.2016.12.038>

693 Furlani, S., Biolchi, S., Cucchi, F., Antonioli, F., Busetti, M., Melis, R., 2011. Tectonic effects on
694 Late Holocene sea level changes in the Gulf of Trieste (NE Adriatic Sea, Italy). *Quaternary
695 International 232*, 144–157. <https://doi.org/10.1016/j.quaint.2010.06.012>

696 Gehrels, W.R., Callard, S.L., Moss, P.T., Marshall, W.A., Blaauw, M., Hunter, J., Milton, J.A.,
697 Garnett, M.H., 2012. Nineteenth and twentieth century sea-level changes in Tasmania and New
698 Zealand. *Earth and Planetary Science Letters 315–316*, 94–102.
699 <https://doi.org/10.1016/j.epsl.2011.08.046>

700 Gehrels, W.R., Hayward, B.W., Newnham, R.M., Southall, K.E., 2008. A 20th century
701 acceleration of sea-level rise in New Zealand. *Geophysical Research Letters 35*, L02717.
702 <https://doi.org/10.1029/2007gl032632>

703 Gehrels, W.R., Kirby, J.R., Prokoph, A., Newnham, R.M., Achterberg, E.P., Evans, H., Black, S.,
704 Scott, D.B., 2005. Onset of recent rapid sea-level rise in the western Atlantic Ocean. *Quaternary*
705 *Science Reviews* 24, 2083–2100. <https://doi.org/10.1016/j.quascirev.2004.11.016>

706 Grenerczy, G., Sella, G., Stein, S., Kenyeres, A., 2005. Tectonic implications of the GPS velocity
707 field in the northern Adriatic region. *Geophys. Res. Lett.* 32, L16311.
708 <https://doi.org/10.1029/2005GL022947>

709 Griffiths, S.D., Hill, D.F., 2015. Tidal modeling, in: Shennan, I., Long, A.J., Horton, B.P. (Eds.),
710 *Handbook of Sea-Level Research*. John Wiley & Sons, Ltd, pp. 438–451.

711 Grinsted, A., Moore, J.C., Jevrejeva, S., 2009. Reconstructing sea level from paleo and projected
712 temperatures 200 to 2100. *Clim Dyn* 34, 461–472. <https://doi.org/10.1007/s00382-008-0507-2>

713 Haslett, J., Parnell, A., 2008. A simple monotone process with application to radiocarbon-dated
714 depth chronologies. *Journal of the Royal Statistical Society: Series C (Applied Statistics)* 57, 399–
715 418. <https://doi.org/10.1111/j.1467-9876.2008.00623.x>

716 Herak, D., Herak, M., Prelogović, E., Markušić, S., Markulin, Ž., 2005. Jabuka island (Central
717 Adriatic Sea) earthquakes of 2003. *Tectonophysics* 398, 167–180.
718 <https://doi.org/10.1016/j.tecto.2005.01.007>

719 Herak, D., Sović, I., Cecić, I., Živčić, M., Dasović, I., Herak, M., 2017. Historical Seismicity of
720 the Rijeka Region (Northwest External Dinarides, Croatia)—Part I: Earthquakes of 1750, 1838,
721 and 1904 in the Bakar Epicentral Area. *Seismological Research Letters* 88, 904–915.
722 <https://doi.org/10.1785/0220170014>

723 Herak, M., Herak, D., Markušić, S., 1996. Revision of the earthquake catalogue and seismicity of
724 Croatia, 1908–1992. *Terra Nova* 8, 86–94. <https://doi.org/10.1111/j.1365-3121.1996.tb00728.x>

725 Hill, D.F., Griffiths, S.D., Peltier, W.R., Horton, B.P., Törnqvist, T.E., 2011. High-resolution
726 numerical modeling of tides in the western Atlantic, Gulf of Mexico, and Caribbean Sea during
727 the Holocene. *J. Geophys. Res.* 116, C10014. <https://doi.org/10.1029/2010JC006896>

728 Horton, B.P., Edwards, R.J., 2006. Quantifying Holocene Sea Level Change Using Intertidal
729 Foraminifera: Lessons from the British Isles. Cushman Foundation for Foraminiferal Research,
730 Special Publication 40, 97.

731 Horton, B.P., Engelhart, S.E., Hill, D.F., Kemp, A.C., Nikitina, D., Miller, K.G., Peltier, W.R.,
732 2013. Influence of tidal-range change and sediment compaction on Holocene relative sea-level
733 change in New Jersey, USA. *J. Quaternary Sci.* 28, 403–411. <https://doi.org/10.1002/jqs.2634>

734 Horton, B.P., Shennan, I., 2009. Compaction of Holocene strata and the implications for relative
735 sealevel change on the east coast of England. *Geology* 37, 1083–1086.
736 <https://doi.org/10.1130/G30042A.1>

737 Hydrographic Institute, 1955. Report on sea level measurement along the eastern Adriatic coast.
738 Split.

739 Jevrejeva, S., Grinsted, A., Moore, J.C., 2009. Anthropogenic forcing dominates sea level rise
740 since 1850. *Geophysical Research Letters* 36. <https://doi.org/10.1029/2009GL040216>

741 Kaufman, L., Rousseeuw, P.J., 1990. Partitioning Around Medoids (Program PAM), in: *Finding*
742 *Groups in Data*. John Wiley & Sons, Inc., pp. 68–125. <https://doi.org/10.1002/9780470316801.ch2>

743 Kemp, A.C., Hawkes, A.D., Donnelly, J.P., Vane, C.H., Horton, B.P., Hill, T.D., Anisfeld, S.C.,
744 Parnell, A.C., Cahill, N., 2015. Relative sea-level change in Connecticut (USA) during the last
745 2200 yrs. *Earth and Planetary Science Letters* 428, 217–229.
746 <https://doi.org/10.1016/j.epsl.2015.07.034>

747 Kemp, A.C., Horton, B.P., Culver, S.J., Corbett, D.R., van de Plassche, O., Gehrels, W.R.,
748 Douglas, B.C., Parnell, A.C., 2009. Timing and magnitude of recent accelerated sea-level rise
749 (North Carolina, United States). *Geology* 37, 1035–1038. <https://doi.org/10.1130/g30352a.1>

750 Kemp, A.C., Horton, B.P., Donnelly, J.P., Mann, M.E., Vermeer, M., Rahmstorf, S., 2011. Climate
751 related sea-level variations over the past two millennia. *Proceedings of the National Academy of*
752 *Sciences*. <https://doi.org/10.1073/pnas.1015619108>

753 Kemp, A.C., Horton, B.P., Vane, C.H., Bernhardt, C.E., Corbett, D.R., Engelhart, S.E., Anisfeld,
754 S.C., Parnell, A.C., Cahill, N., 2013. Sea-level change during the last 2500 years in New Jersey,
755 USA. *Quaternary Science Reviews* 81, 90–104. <https://doi.org/10.1016/j.quascirev.2013.09.024>

756 Kemp, A.C., Kegel, J.J., Culver, S.J., Barber, D.C., Mallinson, D.J., Leorri, E., Bernhardt, C.E.,
757 Cahill, N., Riggs, S.R., Woodson, A.L., Mulligan, R.P., Horton, B.P., 2017. Extended late
758 Holocene relative sea-level histories for North Carolina, USA. *Quaternary Science Reviews* 160,
759 13–30. <https://doi.org/10.1016/j.quascirev.2017.01.012>

760 Kemp, A.C., Nelson, A.R., Horton, B.P., 2013. 14.31 Radiocarbon Dating of Plant Macrofossils
761 from Tidal-Marsh Sediment, in: Shroder, J.F. (Ed.), *Treatise on Geomorphology*. Academic Press,
762 San Diego, pp. 370–388.

763 Kopp, R.E., Kemp, A.C., Bittermann, K., Horton, B.P., Donnelly, J.P., Gehrels, W.R., Hay, C.C.,
764 Mitrovica, J.X., Morrow, E.D., Rahmstorf, S., 2016. Temperature-driven global sea-level
765 variability in the Common Era. *PNAS* 113, E1434–E1441.
766 <https://doi.org/10.1073/pnas.1517056113>

767 Korbar, T., 2009. Orogenic evolution of the External Dinarides in the NE Adriatic region: a model
768 constrained by tectonostratigraphy of Upper Cretaceous to Paleogene carbonates. *Earth-Science*
769 *Reviews* 96, 296–312. <https://doi.org/10.1016/j.earscirev.2009.07.004>

770 Lambeck, K., Anzidei, M., Antonioli, F., Benini, A., Esposito, A., 2004a. Sea level in Roman time
771 in the Central Mediterranean and implications for recent change. *Earth and Planetary Science*
772 *Letters* 224, 563–575. <https://doi.org/10.1016/j.epsl.2004.05.031>

773 Lambeck, K., Antonioli, F., Purcell, A., Silenzi, S., 2004b. Sea-level change along the Italian coast
774 for the past 10,000 yr. *Quaternary Science Reviews* 23, 1567–1598.
775 <https://doi.org/10.1016/j.quascirev.2004.02.009>

776 Lambeck, K., Purcell, A., 2005. Sea-level change in the Mediterranean Sea since the LGM: model
777 predictions for tectonically stable areas. *Quaternary Science Reviews* 24, 1969–1988.
778 <https://doi.org/10.1016/j.quascirev.2004.06.025>

779 Lambeck, K., Antonioli, F., Anzidei, M., Ferranti, L., Leoni, G., Scicchitano, G., Silenzi, S., 2011.
780 Sea level change along the Italian coast during the Holocene and projections for the future.
781 *Quaternary International* 232, 250–257. <https://doi.org/10.1016/j.quaint.2010.04.026>

782 Lambeck, K., Rouby, H., Purcell, A., Sun, Y., Sambridge, M., 2014. Sea level and global ice
783 volumes from the Last Glacial Maximum to the Holocene. *PNAS* 111, 15296–15303.
784 <https://doi.org/10.1073/pnas.1411762111>

785 Mann, M.E., Zhang, Z., Rutherford, S., Bradley, R.S., Hughes, M.K., Shindell, D., Ammann, C.,
786 Faluvegi, G., Ni, F., 2009. Global Signatures and Dynamical Origins of the Little Ice Age and
787 Medieval Climate Anomaly. *Science* 326, 1256–1260. <https://doi.org/10.1126/science.1177303>

788 Marcos, M., Tsimplis, M.N., 2008. Coastal sea level trends in Southern Europe. *Geophysical*
789 *Journal International* 175, 70–82.

790 Marcott, S.A., Shakun, J.D., Clark, P.U., Mix, A.C., 2013. A Reconstruction of Regional and
791 Global Temperature for the Past 11,300 Years. *Science* 339, 1198–1201.
792 <https://doi.org/10.1126/science.1228026>

793 Marriner, N., Morhange, C., Faivre, S., Flaux, C., Vacchi, M., Miko, S., Dumas, V., Boetto, G.,
794 Radic Rossi, I., 2014. Post-Roman sea-level changes on Pag Island (Adriatic Sea): Dating
795 Croatia's "enigmatic" coastal notch? *Geomorphology* 221, 83–94.
796 <https://doi.org/10.1016/j.geomorph.2014.06.002>

797 Marriner, N., Kaniewski, D., Morhange, C., Flaux, C., Giaime, M., Vacchi, M., Goff, J., 2017.
798 Tsunamis in the geological record: Making waves with a cautionary tale from the Mediterranean.
799 *Science Advances* 3, e1700485. <https://doi.org/10.1126/sciadv.1700485>

800 Marjanović, M., Bačić, Ž., Bačić, T., 2012. Determination of Horizontal and Vertical Movements
801 of the Adriatic Microplate on the Basis of GPS Measurements, in: Kenyon, S., Pacino, M.C., Marti,
802 U. (Eds.), *Geodesy for Planet Earth, International Association of Geodesy Symposia*. Springer
803 Berlin Heidelberg, pp. 683–688.

804 Marshall, W., 2015. Chronohorizons, in: Shennan, I., Long, A.J., Horton, B.P. (Eds.), *Handbook*
805 *of Sea-Level Research*. John Wiley & Sons, Ltd, pp. 373–385.
806 <https://doi.org/10.1002/9781118452547.ch25>

807 McKenzie, D., 1972. Active Tectonics of the Mediterranean Region. *Geophysical Journal*
808 *International* 30, 109–185. <https://doi.org/10.1111/j.1365-246X.1972.tb02351.x>

809 Oldow, J.S., Ferranti, L., Lewis, D.S., Campbell, J.K., D'Argenio, B., Catalano, R., Pappone, G.,
810 Carmignani, L., Conti, P., Aiken, C.L.V., 2002. Active fragmentation of Adria, the north African
811 promontory, central Mediterranean orogen. *Geology* 30, 779–782. [https://doi.org/10.1130/0091-](https://doi.org/10.1130/0091-7613(2002)030<0779:AFOATN>2.0.CO;2)
812 [7613\(2002\)030<0779:AFOATN>2.0.CO;2](https://doi.org/10.1130/0091-7613(2002)030<0779:AFOATN>2.0.CO;2)

813 Orlić, M., Gačić, M., La Violette, P.E., 1992. The currents and circulation of the Adriatic Sea.
814 *Oceanologica Acta* 15, 109–124.

815 Orlić, M., Kuzmić, M., Pasarić, Z., 1994. Response of the Adriatic Sea to the bora and sirocco
816 forcing. *Continental Shelf Research* 14, 91–116. [https://doi.org/10.1016/0278-4343\(94\)90007-8](https://doi.org/10.1016/0278-4343(94)90007-8)

817 Orlić, M., Pašarić, M., 2000. Sea-level changes and crustal movements recorded along the east
818 Adriatic coast. *Nuovo cimento della Società italiana di fisica. C* 23, 351–364.

819 Pandža, M., Franjić, J., Škvorc, Ž., 2007. The salt marsh vegetation on the East Adriatic coast.
820 *Biologia* 62, 24–31. <https://doi.org/10.2478/s11756-007-0003-x>

821 Parnell, A.C., Haslett, J., Allen, J.R.M., Buck, C.E., Huntley, B., 2008. A flexible approach to
822 assessing synchronicity of past events using Bayesian reconstructions of sedimentation history.
823 *Quaternary Science Reviews* 27, 1872–1885. <https://doi.org/10.1016/j.quascirev.2008.07.009>

824 Peltier, W.R., Argus, D.F., Drummond, R., 2015. Space geodesy constrains ice age terminal
825 deglaciation: The global ICE-6G_C (VM5a) model. *J. Geophys. Res. Solid Earth* 120,
826 2014JB011176. <https://doi.org/10.1002/2014JB011176>

827 Pirazzoli, P., 1996. *Sea Level Changes. The Last 20 000 Years*. John Wiley & Sons Ltd,
828 Chichester, New York.

829 Pirazzoli, P.A., 2005. A review of possible eustatic, isostatic and tectonic contributions in eight
830 Late-Holocene relative sea-level histories from the Mediterranean area. *Quaternary Science*
831 *Reviews, Quaternary coastal morphology and sea-level changes* 24, 1989–2001.
832 <https://doi.org/10.1016/j.quascirev.2004.06.026>

833 Pirazzoli, P.A., 1991. *World Atlas of Holocene Sea-Level Changes*, 1st ed. Elsevier.

834 Pirazzoli, P.A., 1976. Sea Level Variations in the Northwest Mediterranean During Roman Times.
835 *Science* 194, 519–521. <https://doi.org/10.1126/science.194.4264.519>

836 Plater, A.J., Kirby, J.R., Boyle, J.F., Shaw, T., Mills, H., 2015. Loss on ignition and organic
837 content, in: Shennan, I., Long, A.J., Horton, B.P. (Eds.), Handbook of Sea-Level Research. John
838 Wiley & Sons, Ltd, pp. 312–330.

839 Reimer, P.J., Bard, E., Bayliss, A., Beck, J.W., Blackwell, P.G., Bronk Ramsey, C., Buck, C.E.,
840 Cheng, H., Edwards, R.L., Friedrich, M., Grootes, P.M., Guilderson, T.P., Haflidason, H., Hajdas,
841 I., Hatté, C., Heaton, T.J., Hoffmann, D.L., Hogg, A.G., Hughen, K.A., Kaiser, K.F., Kromer, B.,
842 Manning, S.W., Niu, M., Reimer, R.W., Richards, D.A., Scott, E.M., Southon, J.R., Staff, R.A.,
843 Turney, C.S.M., van der Plicht, J., 2013. IntCal13 and Marine13 Radiocarbon Age Calibration
844 Curves 0–50,000 Years cal BP. Radiocarbon; Vol 55, No 4 (2013).

845 Rosenthal, Y., Kalansky, J., Morley, A., Linsley, B., 2017. A paleo-perspective on ocean heat
846 content: Lessons from the Holocene and Common Era. Quaternary Science Reviews 155, 1–12.
847 <https://doi.org/10.1016/j.quascirev.2016.10.017>

848 Roy, K., Peltier, W.R., 2017. Space-geodetic and water level gauge constraints on continental
849 uplift and tilting over North America: regional convergence of the ICE-6G_C (VM5a/VM6)
850 models. Geophys J Int 210, 1115–1142. <https://doi.org/10.1093/gji/ggx156>

851 Roy, K., Peltier, W.R., 2018. Relative sea level in the Western Mediterranean basin: A regional
852 test of the ICE-7G_NA (VM7) model and a constraint on late Holocene Antarctic deglaciation.
853 Quaternary Science Reviews 183, 76–87. <https://doi.org/10.1016/j.quascirev.2017.12.021>

854 Saher, M.H., Gehrels, W.R., Barlow, N.L.M., Long, A.J., Haigh, I.D., Blaauw, M., 2015. Sea-
855 level changes in Iceland and the influence of the North Atlantic Oscillation during the last half
856 millennium. Quaternary Science Reviews 108, 23–36.
857 <https://doi.org/10.1016/j.quascirev.2014.11.005>

858 Scott, D.B., Hermelin, J.O.R., 1993. A Device for Precision Splitting of Micropaleontological
859 Samples in Liquid Suspension. *Journal of Paleontology* 67, 151–154.
860 <https://doi.org/10.2307/1305976>

861 Scott, D.B., Medioli, F.S., 1980. Quantitative studies of marsh foraminiferal distributions in nova-
862 scotia canada implications for sea level studies. Cushman Foundation for Foraminiferal Research
863 Special Publication 1–58.

864 Scott, D.B., Medioli, F.S., 1978. Vertical zonations of marsh foraminifera as accurate indicators
865 of former sea-levels. *Nature* 272, 528–531. <https://doi.org/10.1038/272528a0>

866 Serpelloni, E., Faccenna, C., Spada, G., Dong, D., Williams, S.D.P., 2013. Vertical GPS ground
867 motion rates in the Euro-Mediterranean region: New evidence of velocity gradients at different
868 spatial scales along the Nubia-Eurasia plate boundary. *J. Geophys. Res. Solid Earth* 118,
869 2013JB010102. <https://doi.org/10.1002/2013JB010102>

870 Shaw, T.A., Kirby, J.R., Holgate, S., Tutman, P., Plater, A.J., 2016. Contemporary salt-marsh
871 foraminiferal distribution from the Adriatic coast of Croatia and its potential for sea-level studies.
872 *Journal of Foraminiferal Research* 46, 314–332. <https://doi.org/10.2113/gsjfr.46.3.314>

873 Sivan, D., Lambeck, K., Toueg, R., Raban, A., Porath, Y., Shirman, B., 2004. Ancient coastal
874 wells of Caesarea Maritima, Israel, an indicator for relative sea level changes during the last 2000
875 years. *Earth and Planetary Science Letters* 222, 315–330.
876 <https://doi.org/10.1016/j.epsl.2004.02.007>

877 Spada, G., Stocchi, P., Colleoni, F., 2009. Glacio–isostatic Adjustment in the Po Plain and in the
878 Northern Adriatic Region. *Pure and Applied Geophysics* 166, 1303–1318.
879 <https://doi.org/10.1007/s00024-004-0498-9>

880 Šparica, M., Bačani, A., Koch, G., Anda, A., Miko, S., Viličić, D., Galovć, I., Šparica, M., M.,
881 Ibrahimpšarić, H., Bargant, S., Dolenc, T., 2005. Ecosystem of Morinje Bay (Adriatic Sea,
882 Croatia): Aspects of the sediment/water interface. *RMZ - Materials and Geoenvironment* 52, 115–
883 118.

884 Stocchi, P., Spada, G., 2007. Glacio and hydro-isostasy in the Mediterranean Sea: Clark's zones
885 and role of remote ice sheets. *Annals of Geophysics* 50, 741–761.

886 Stocchi, P., Spada, G., 2009. Influence of glacial isostatic adjustment upon current sea level
887 variations in the Mediterranean. *Tectonophysics* 474, 56–68.
888 <https://doi.org/10.1016/j.tecto.2009.01.003>

889 Strachan, K.L., Finch, J.M., Hill, T.R., Barnett, R.L., 2014. A late Holocene sea-level curve for
890 the east coast of South Africa. *South African Journal of Science* 110, 9 Pages.
891 <https://doi.org/10.1590/sajs.2014/20130198>

892 Surić, M., Korbar, T., Juračić, M., 2014. Tectonic constraints on the late Pleistocene-Holocene
893 relative sea-level change along the north-eastern Adriatic coast (Croatia). *Geomorphology* 220,
894 93–103. <https://doi.org/10.1016/j.geomorph.2014.06.001>

895 Toker, E., Sivan, D., Stern, E., Shirman, B., Tsimplis, M., Spada, G., 2012. Evidence for centennial
896 scale sea level variability during the Medieval Climate Optimum (Crusader Period) in Israel,
897 eastern Mediterranean. *Earth and Planetary Science Letters, Sea Level and Ice Sheet Evolution: A*
898 *PALSEA Special Edition* 315–316, 51–61. <https://doi.org/10.1016/j.epsl.2011.07.019>

899 Törnqvist, T.E., Rosenheim, B.E., Hu, P., Fernandez, A.B., 2015. Radiocarbon dating and
900 calibration, in: Shennan, I., Long, A.J., Horton, B.P. (Eds.), *Handbook of Sea-Level Research*.
901 John Wiley & Sons, Ltd, pp. 347–360.

902 Törnqvist, T.E., Wallace, D.J., Storms, J.E.A., Wallinga, J., van Dam, R.L., Blaauw, M., Derksen,
903 M.S., Klerks, C.J.W., Meijneken, C., Snijders, E.M.A., 2008. Mississippi Delta subsidence
904 primarily caused by compaction of Holocene strata. *Nature Geosci* 1, 173–176.
905 <https://doi.org/10.1038/ngeo129>

906 Troëls-Smith, J., 1955. Characterization of unconsolidated sediments. *Danmarks Geologiske*
907 *Undersøgelse Series* 4, 1–73.

908 Tsimplis, M.N., Baker, T.F., 2000. Sea level drop in the Mediterranean Sea: An indicator of deep
909 water salinity and temperature changes? *Geophysical Research Letters* 27, 1731–1734.
910 <https://doi.org/10.1029/1999gl007004>

911 Tsimplis, M.N., Josey, S.A., 2001. Forcing of the Mediterranean Sea by atmospheric oscillations
912 over the North Atlantic. *Geophysical Research Letters* 28, 803–806.
913 <https://doi.org/10.1029/2000gl012098>

914 Tsimplis, M.N., Raicich, F., Fenoglio-Marc, L., Shaw, A.G.P., Marcos, M., Somot, S.,
915 Bergamasco, A., 2012. Recent developments in understanding sea level rise at the Adriatic coasts.
916 *Physics and Chemistry of the Earth, Parts A/B/C* 40–41, 59–71.
917 <https://doi.org/10.1016/j.pce.2009.11.007>

918 Vacchi, M., Marriner, N., Morhange, C., Spada, G., Fontana, A., Rovere, A., 2016. Multiproxy
919 assessment of Holocene relative sea-level changes in the western Mediterranean: Sea-level
920 variability and improvements in the definition of the isostatic signal. *Earth-Science Reviews* 155,
921 172–197. <https://doi.org/10.1016/j.earscirev.2016.02.002>

922 Van De Plassche, O., Wright, A.J., Horton, B.P., Engelhart, S.E., Kemp, A.C., Mallinson, D.,
923 Kopp, R.E., 2014. Estimating tectonic uplift of the Cape Fear Arch (south-eastern United States)

924 using reconstructions of Holocene relative sea level. *J. Quaternary Sci.* 29, 749–759.
925 <https://doi.org/10.1002/jqs.2746>

926 Vilibić, I., 2006. The role of the fundamental seiche in the Adriatic coastal floods. *Continental*
927 *Shelf Research* 26, 206–216. <https://doi.org/10.1016/j.csr.2005.11.001>

928 Vilibić, I., Orlić, M., Čupić, S., Domijan, N., Leder, N., Mihanović, H., Pasarić, M., Pasarić, Z.,
929 Srđelić, M., Strinić, G., 2005. A new approach to sea level observations in Croatia. *Geofizika* 22,
930 21–57.

931 Vilibić, I., Šepić, J., 2009. Destructive meteotsunamis along the eastern Adriatic coast: Overview.
932 *Physics and Chemistry of the Earth, Parts A/B/C* 34, 904–917.
933 <https://doi.org/10.1016/j.pce.2009.08.004>

934 Vilibić, I., Šepić, J., Pasarić, M., Orlić, M., 2017. The Adriatic Sea: A Long-Standing Laboratory
935 for Sea Level Studies. *Pure Appl. Geophys.* 174, 3765–3811. [https://doi.org/10.1007/s00024-017-](https://doi.org/10.1007/s00024-017-1625-8)
936 [1625-8](https://doi.org/10.1007/s00024-017-1625-8)

937 Weber, J., Vrabc, M., Pavlovcic-Preseren, P., Dixon, T., Jiang, Y., Stopar, B., 2010. GPS-derived
938 motion of the Adriatic microplate from Istria Peninsula and Po Plain sites, and geodynamic
939 implications. *Tectonophysics* 483, 214–222. <https://doi.org/10.1016/j.tecto.2009.09.001>

940 Williams, C.K.I., Rasmussen, C.E., 1996. *Gaussian Processes for Regression*. MIT Press,
941 Cambridge.

942 Woodworth, P.L., 2003. Some Comments on the Long Sea Level Records from the Northern
943 Mediterranean. *Journal of Coastal Research* 19, 212–217.

944 Zerbini, S., Plag, H.-P., Baker, T., Becker, M., Billiris, H., Bürki, B., Kahle, H.-G., Marson, I.,
945 Pezzoli, L., Richter, B., Romagnoli, C., Sztobryn, M., Tomasi, P., Tsimplis, M., Veis, G., Verrone,
946 G., 1996. Sea level in the Mediterranean: a first step towards separating crustal movements and

947 absolute sea-level variations. *Global and Planetary Change* 14, 1–48.
948 [https://doi.org/10.1016/0921-8181\(96\)00003-3](https://doi.org/10.1016/0921-8181(96)00003-3)
949 Zerbini, S., Raicich, F., Prati, C.M., Bruni, S., Del Conte, S., Errico, M., Santi, E., 2017. Sea-level
950 change in the Northern Mediterranean Sea from long-period tide gauge time series. *Earth-Science*
951 *Reviews* 167, 72–87. <https://doi.org/10.1016/j.earscirev.2017.02.009>